NATIONAL ADVISORY COMMITTEE FOR AERONAUTICS

TECHNICAL NOTE 3737

THE MOTIONS OF ROLLING SYMMETRICAL MISSILES REFERRED TO A BODY-AXIS SYSTEM

By Robert L. Nelson

Langley Aeronautical Laboratory
Langley Field, Va.

Washington
November 1956

NATIONAL ADVISORY COMMITTEE FOR AERONAUTICS

TECHNICAL NOTE 3737

THE MOTIONS OF ROLLING SYMMETRICAL MISSILES REFERRED TO A BODY-AXIS SYSTEM

By Robert L. Nelson

SUMMARY

The linearized equations of motion have been derived for a rolling missile having slight aerodynamic asymmetries. Time histories of rolling-missile motions referred to a body-axis system have been prepared to show the types of missile motions that can be encountered. The motions resulting from a trim change and a pulse-rocket disturbance are shown to be determined mainly by the ratio of rolling velocity to pitching frequency.

Finally, the derived equations are used in establishing a technique for the reduction of rolling-missile oscillation data. It is shown that the aerodynamic derivatives can be obtained from flight data if four accelerations are measured. The method is applied to the results obtained from a flight test of a missile configuration.

INTRODUCTION

The problem of the dynamic stability of missiles has been attacked by two separate basic treatments. First, in the case of roll-stabilized missiles the problem has been attacked by means of the classical airplane-stability theory developed by Lanchester (ref. 1), with no need for modifications. The development of the theory for rolling symmetrical missiles has followed from the basic ballistic theory of reference 2. Nicolaides (ref. 3) and Charters (ref. 4) have more recently expressed the dynamic-stability equations for rolling symmetrical missiles in terminology more familiar to the aerodynamicist. However, the impetus for these works was provided by studies of missile motions in aerodynamic test ranges where the model position and angular orientations were measured at a series of stations. As a result the equations derived were referred to space axes. In the case of free-flight rolling missiles equipped with internal instrumentation, the equations of motion must be referred to a body-axis system. Phillips in reference 5 presented a simplified analysis of the motion of rolling airplanes (and in a limiting case of symmetrical missiles) based on a body-axis system but included only the criteria for stability. Bolz in reference 6 derived more completely the equations of motion for a rolling

symmetrical missile referred to a body-axis system but again discussed only the criteria for stability.

In this paper the equations of motion referenced to the body-axis system are again derived, and assumptions similar to those of Nicolaides (ref. 3) are used. Some of the possible missile motions are shown, together with the motions to be expected from certain forcing functions. Finally, the derived equations of motion are used to establish a technique for the reduction of oscillation data to obtain aerodynamic derivatives. The method is applied to the experimental results obtained from a rolling symmetrical missile.

SYMBOLS

a resultant acceleration

a, b complex roots of differential equation for ζ

a_X, a_Y, a_Z accelerations parallel to X, Y, and Z axes, respectively

A, B, C constants of differential equation for ζ

A_F body frontal area, sq ft

C_m pitching-moment coefficient, $\frac{M_Y}{qA_F d}$

$C_{m_\alpha} = \frac{\partial C_m}{\partial \alpha}$

$C_{m_q} = \frac{\partial C_m}{\partial \frac{\dot{\theta} d}{2V}}$

$C_{m_{\dot{\theta}}} = \frac{\partial C_m}{\partial \dot{\theta}}$, sec

$C_{m_{\dot{\phi}_\beta}} = \frac{\partial C_m}{\partial \dot{\phi} \partial \beta}$, sec

C_N normal-force coefficient ($-C_Z$)

$C_{N_\alpha} = \frac{\partial C_N}{\partial \alpha} = -\frac{\partial C_Z}{\partial \alpha}$

C_n yawing-moment coefficient, $\frac{M_Z}{qA_F d}$

$C_{n_\beta} = \frac{\partial C_n}{\partial \beta}$

$C_{n_{\dot{\psi}}} = \frac{\partial C_n}{\partial \dot{\psi}}$, sec

$C_{n_{\dot{\phi}_\alpha}} = \frac{\partial C_n}{\partial \dot{\phi} \partial \alpha}$, sec

$C_{n_{p_\alpha}} = \frac{\partial C_n}{\partial \left(\frac{\dot{\phi} d}{2V}\right) \partial \alpha}$

C_R magnitude of resultant vector

$C_{R,o} = R_1 + R_2$

C_Y lateral-force coefficient, $\frac{F_Y}{qA_F}$

$C_{Y,o}$ lateral-force coefficient due to asymmetry

$C_{Y_\beta} = \frac{\partial C_Y}{\partial \beta}$

C_Z vertical-force coefficient, $\frac{F_Z}{qA_F}$

$C_{Z,o}$ vertical-force coefficient due to asymmetry

$C_{Z_\alpha} = \frac{\partial C_Z}{\partial \alpha}$

d body diameter, ft

F_X, F_Y, F_Z aerodynamic forces parallel to X, Y, and Z axes, respectively

I moment of inertia about Y- or Z-axis, slug-ft^2

$I' = \frac{I}{qA_F d}$, sec^2

I_X	moment of inertia about X-axis, slug-ft^2
$i = \sqrt{-1}$	
$K = \frac{R_1 - R_2}{R_1 + R_2}$	
k	radius of gyration, $\sqrt{I/m}$, ft
l	pulse-rocket moment arm from center of gravity, ft
M_X, M_Y, M_Z	aerodynamic moments about X, Y, and Z axes, respectively
m	mass, slug
$m' = \frac{mu}{qA_F}$, sec	
P	pulse-rocket total impulse, lb-sec
p	rolling velocity, radians/sec
q	dynamic pressure, lb/sq ft
R_1, R_2	initial magnitude of rotating vectors
s	slope
t	time
u	component of free-stream velocity in X-direction, ft/sec ($u \approx V$)
V	free-stream velocity, ft/sec
X, Y, Z	coordinate axes
x_o	longitudinal center of pressure of asymmetric force, ft
x_1, x_2	longitudinal displacement of accelerometers, ft
y_1, y_2	lateral displacement of accelerometers, ft
z_1, z_2	vertical displacement of accelerometers, ft

α	angle of attack, radians
β	angle of sideslip, radians
$\zeta = \beta + i\alpha$	
$\dot{\theta}$	pitching velocity, radians/sec
Λ	angular orientation of resultant vector, radians
$\Lambda_o = \nu_1 = \nu_2$,	radians
λ_o	nonrolling damping constant, 1/sec
$\Delta\lambda$	damping constant due to roll, 1/sec
μ	relative-density factor, $\frac{4m}{\rho A_F d}$
ν_1, ν_2	initial angular orientation of rotating vectors, radians
ρ	air density, slugs/cu ft
$\dot{\phi}$	rolling velocity, radians/sec
$\dot{\psi}$	yawing velocity, radians/sec
ω_o	basic oscillation frequency, radians/sec
$\Delta\omega$	component of total pitch frequency resulting directly from roll, radians/sec
$\Omega = \dot{\theta} + i\dot{\psi}$	

Dots over symbols indicate time derivatives.

STATEMENT OF THE PROBLEM

The motion of a symmetrical missile configuration referred to a body-axis system is complicated by rolling motion even for the case where the rolling velocity is a fraction of the missile pitching frequency. Unlike the motion of a slowly rolling airplane-like configuration which tends to continue in a direction normal to the wing plane, the motion of a symmetrical missile configuration disturbed in one plane in space tends to remain in one plane in space. (The restoring force for the airplane is normal to the plane of the wings, whereas the restoring force for the missile is

mainly independent of roll attitude.) Thus for a missile having accelerometers mounted at the center of gravity the first consequence of the rolling motion is the appearance of a roll effect on the normal and transverse accelerometer traces. An example of this effect for the normal-accelerometer trace is shown in the following sketch:

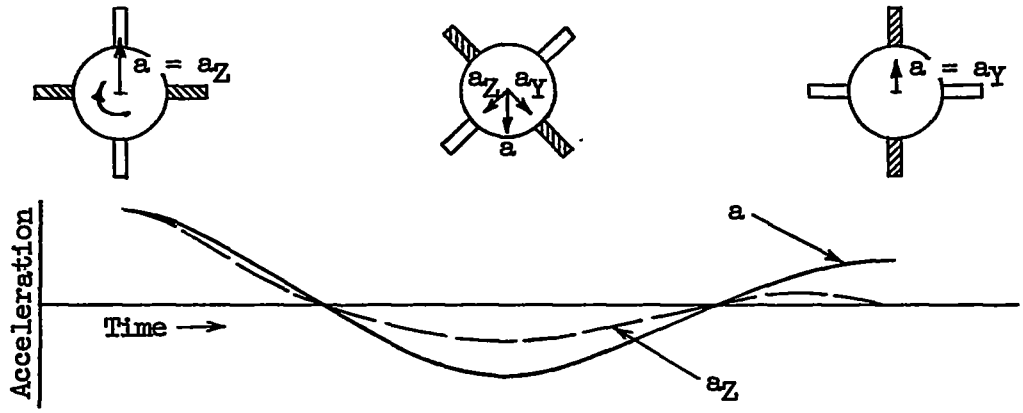

This roll effect is determined mainly by the ratio of the rolling velocity to the oscillation frequency, or the ratio of $pd/2V$ to $\omega_o d/2V$. At very low values of $pd/2V$ corresponding to very small fin misalinements, this ratio can become large if the missile ascends to a high altitude, inasmuch as $pd/2V$ is independent of altitude while $\omega_o d/2V$ decreases with increasing altitude.

If the missile motion were in one plane in space and the roll rate small, the motion could be analyzed simply by working with the resultant of normal and transverse acceleration, and applying the usual data-reduction techniques for oscillating nonrolling models (ref. 7). However, since the missile may not remain in one plane in space and gyroscopic cross-coupling can have a large effect on the model motion, an analysis of the motions of rolling missiles is necessary in order to interpret and reduce the flight test data.

DEVELOPMENT OF EQUATIONS OF MOTION

The linearized equations of motion for a symmetrical missile (90° rotational symmetry) are referred to the body-axis system of the following sketch:

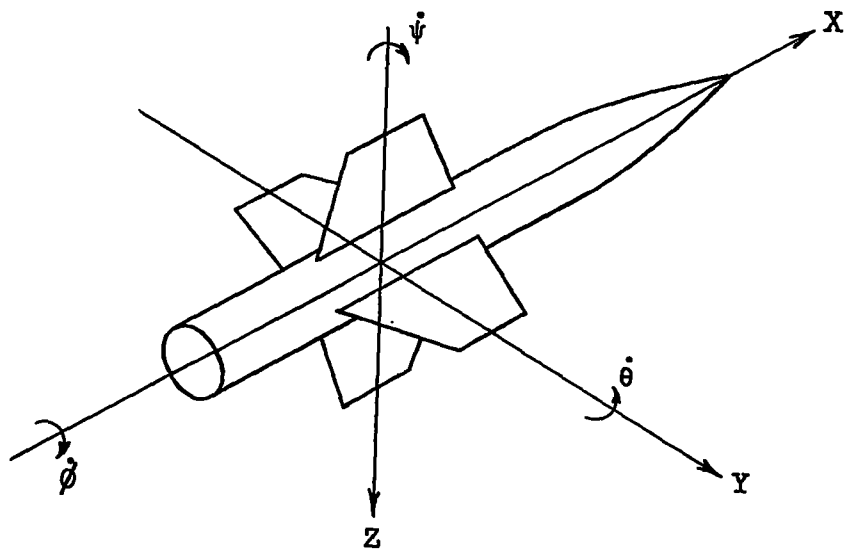

On the assumption that angular deviations from trim are small but that large rolling velocity must be considered, the equations of motion reduce to

$$ma_X = \Sigma F_X$$

$$mu(\dot{\beta} + \dot{\psi} - \dot{\phi}\alpha) = \Sigma F_Y$$

$$mu(\dot{\alpha} - \dot{\theta} + \dot{\phi}\beta) = \Sigma F_Z$$

$$I_X\ddot{\phi} = \Sigma M_X$$

$$I\ddot{\theta} - (I - I_X)\dot{\phi}\dot{\psi} = \Sigma M_Y$$

$$I\ddot{\psi} + (I - I_X)\dot{\phi}\dot{\theta} = \Sigma M_Z$$

u = component of free-stream velocity in x-direction

If the forward velocity is assumed to be constant ($a_X = 0$) and the rolling velocity also to be constant ($\ddot{\phi} = 0$), the equations reduce to the following four:

$$mu(\dot{\beta} + \dot{\psi} - \dot{\phi}\alpha) = \Sigma F_Y \tag{1}$$

$$mu(\dot{\alpha} - \dot{\theta} + \dot{\phi}\beta) = \Sigma F_Z \tag{2}$$

$$I\ddot{\theta} - (I - I_X)\dot{\phi}\dot{\psi} = \Sigma M_Y \tag{3}$$

$$I\ddot{\psi} + (I - I_X)\dot{\phi}\dot{\theta} = \Sigma M_Z \tag{4}$$

In order to reduce the number of equations to two, equations (2) and (4) are multiplied by $i = \sqrt{-1}$ and added to equations (1) and (3), respectively, to obtain

$$mu\left[(\dot{\beta} + i\dot{\alpha}) - i(\dot{\theta} + i\dot{\psi}) + i\dot{\phi}(\beta + i\alpha)\right] = \Sigma(F_Y + iF_Z)$$

$$I(\ddot{\theta} + i\ddot{\psi}) + i\dot{\phi}(I - I_X)(\dot{\theta} + i\dot{\psi}) = \Sigma(M_Y + iM_Z)$$

Let $\zeta = \beta + i\alpha$, $\Omega = \dot{\theta} + i\dot{\psi}$, and $\dot{\phi} = p$ so that these equations become:

$$\dot{\zeta} + ip\zeta - i\Omega = \frac{\Sigma(F_Y + iF_Z)}{mu} \tag{5}$$

$$\dot{\Omega} + ip\left(1 - \frac{I_X}{I}\right)\Omega = \frac{\Sigma(M_Y + iM_Z)}{I} \tag{6}$$

Allowing small asymmetries (resulting from a fixed control deflection for example) which do not violate the assumption of symmetry and assuming that the aerodynamic forces due to $\dot{\psi}$, $\dot{\theta}$, and $\dot{\phi}$, and forces due to gravity are negligible in comparison to the forces due to angle of attack and

sideslip permits the force equations to be written as:

$$\Sigma F_Y = C_{Y_\beta} qA_F \beta + C_{Y_o} qA_F$$

$$\Sigma F_Z = C_{Z_\alpha} qA_F \alpha + C_{Z_o} qA_F$$

Then, multiplying the second equation by i and adding to the first gives

$$\Sigma(F_Y + iF_Z) = qA_F\left(C_{Y_\beta}\beta + iC_{Z_\alpha}\alpha\right) + qA_F\left(C_{Y_o} + iC_{Z_o}\right)$$

From the assumption of symmetry,

$$C_{Y_\beta} = C_{Z_\alpha} = -C_{N_\alpha}$$

The derivative C_{N_α} rather than C_{Y_β} or C_{Z_α} is used hereinafter, since the force due to a positive angle of attack is usually considered positive. Then,

$$\Sigma(F_Y + iF_Z) = -C_{N_\alpha} qA_F(\beta + i\alpha) + qA_F\left(C_{Y_o} + iC_{Z_o}\right)$$

Let $m' = \frac{mu}{qA_F}$; then, inasmuch as $\zeta = \beta + i\alpha$,

$$\frac{\Sigma(F_Y + iF_Z)}{mu} = -\frac{C_{N_\alpha}\zeta}{m'} + \frac{C_{Y_o} + iC_{Z_o}}{m'}$$

If no moments from asymmetries are allowed to result from camber effects and if the moments due to $\dot{\theta}$, $\dot{\psi}$, and $\dot{\phi}$ are assumed to make a significant contribution to the total moment, the moment equations can be written as:

$$\Sigma M_Y = C_{m_\alpha} qA_F d\alpha + C_{m_{\dot{\theta}}} qA_F d\dot{\theta} + C_{m_{\dot{\phi}_\beta}} qA_F d\dot{\phi}\beta - C_{Z_o} x_o qA_F$$

$$\Sigma M_Z = C_{n_\beta} qA_F d\beta + C_{n_{\dot{\psi}}} qA_F d\dot{\psi} + C_{n_{\dot{\phi}_\alpha}} qA_F d\dot{\phi}\alpha + C_{Y_o} x_o qA_F$$

Again, multiplying the second of these equations by i and adding it to the first gives

$$\Sigma(M_Y + iM_Z) = qA_F d\left[\left(C_{m_\alpha}\alpha + iC_{n_\beta}\beta\right) + \left(C_{m_{\dot{\theta}}}\dot{\theta} + iC_{n_{\dot{\psi}}}\dot{\psi}\right) + \left(C_{m_{\dot{\phi}_\beta}}\dot{\phi}\beta + iC_{n_{\dot{\phi}_\alpha}}\dot{\phi}\alpha\right) - \left(C_{Z_o} - iC_{Y_o}\right)\frac{x_o}{d}\right]$$

With the assumption of 90° rotational symmetry,

$$C_{n_\beta} = -C_{m_\alpha}$$

$$C_{n_{\dot{\psi}}} = C_{m_{\dot{\theta}}}$$

$$C_{n_{\dot{\phi}_\alpha}} = C_{m_{\dot{\phi}_\beta}}$$

Then

$$\Sigma(M_Y + iM_Z) = -iqA_F d\left[\left(C_{m_\alpha} + iC_{n_{\dot{\phi}_\alpha}}\dot{\phi}\right)(\beta + i\alpha) + iC_{m_{\dot{\theta}}}(\dot{\theta} + i\dot{\psi}) - \left(C_{Y_o} + iC_{Z_o}\right)\frac{x_o}{d}\right]$$

Also, with $\zeta = \beta + i\alpha$, $\Omega = \dot{\theta} + i\dot{\psi}$, $\dot{\phi} = p$, and $I' = \frac{I}{qA_F d}$,

$$\frac{\Sigma(M_Y + iM_Z)}{I} = -\frac{i}{I'}\left[\left(C_{m_\alpha} + ipC_{n_{\dot{\phi}_\alpha}}\right)\zeta + iC_{m_{\dot{\theta}}}\Omega - \left(C_{Y_o} + iC_{Z_o}\right)\frac{x_o}{d}\right] \tag{8}$$

Equations (5), (6), (7), and (8) combine to give two linear differential equations in terms of the two unknowns ζ and Ω. The following equation in ζ results:

$$\ddot{\zeta} + A\dot{\zeta} - B\zeta = C \tag{9}$$

where

$$A = \frac{C_{N_\alpha}}{m'} - \frac{C_{m_{\dot{\theta}}}}{I'} + ip\left(2 - \frac{I_X}{I}\right) \tag{10}$$

$$B = \frac{C_{m_\alpha}}{I'} + i\frac{C_{n_{\dot{\phi}_\alpha}}}{I'}p + p^2\left(1 - \frac{I_X}{I}\right) + \frac{C_{m_{\dot{\theta}}}}{I'}\frac{C_{N_\alpha}}{m'} - ip\left(\frac{C_{N_\alpha}}{m'} - \frac{C_{m_{\dot{\theta}}}}{I'} - \frac{I_X}{I}\frac{C_{N_\alpha}}{m'}\right) \tag{11}$$

$$C = -\frac{\left(C_{Y_o} + iC_{Z_o}\right)\frac{x_o}{d}}{I'} - \left[\frac{C_{m_{\dot{\theta}}}}{I'} - ip\left(1 - \frac{I_X}{I}\right)\right]\frac{\left(C_{Y_o} + iC_{Z_o}\right)}{m'} \tag{12}$$

The solution of the differential equation is:

$$\zeta = \zeta_{trim} + R_1 e^{i\nu_1} e^{at} + R_2 e^{i\nu_2} e^{bt}$$

where:

$$a = \frac{-A + \sqrt{A^2 + 4B}}{2}$$

$$b = \frac{-A - \sqrt{A^2 + 4B}}{2}$$

$$\zeta_{trim} = -C/B$$

and $R_1 e^{i\nu_1}$ and $R_2 e^{i\nu_2}$ are initial conditions as shown in the adjacent sketch.

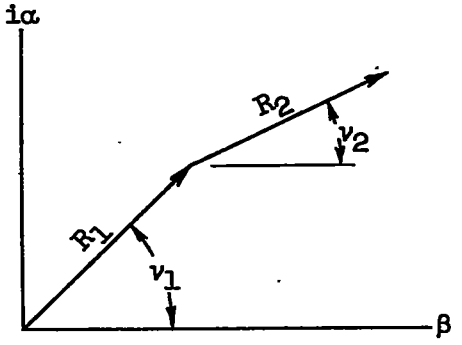

Both a and b are complex numbers, with the complex radical $\sqrt{A^2 + 4B}$, and can be broken down into a more usable form to

$$a = \lambda_o + \Delta\lambda + i(\omega_o - \Delta\omega)$$

$$b = \lambda_o - \Delta\lambda - i(\omega_o + \Delta\omega)$$

where the new concepts λ_o, $\Delta\lambda$, ω_o, and $\Delta\omega$ are defined by

$$\lambda_o = -\frac{1}{2}\left(\frac{C_{N_\alpha}}{m'} - \frac{C_{m_{\dot\theta}}}{I'}\right) \qquad < -\frac{A}{2} \tag{13}$$

$$\omega_o = \frac{1}{2\sqrt{2}}\sqrt{\underbrace{-\frac{4C_{m_\alpha}}{I'} + p^2\frac{I_X^2}{I^2}}_{B^2-4C} - \underbrace{\left(\frac{C_{N_\alpha}}{m'} + \frac{C_{m_{\dot\theta}}}{I'}\right)^2}_{A^2} + \sqrt{\left[-\frac{4C_{m_\alpha}}{I'} + p^2\frac{I_X^2}{I^2} - \left(\frac{C_{N_\alpha}}{m'} + \frac{C_{m_{\dot\theta}}}{I'}\right)^2\right]^2 + 4\left[p\frac{I_X}{I}\left(\frac{C_{N_\alpha}}{m'} + \frac{C_{m_{\dot\theta}}}{I'}\right) + 2p\frac{C_{n_{\dot\phi}\alpha}}{I'}\right]^2}} \tag{14}$$

$$= -(\cdots)$$

$$\Delta\lambda = \frac{1}{4\omega_o}\, p\, \frac{I_X}{I}\left(\frac{C_{N_\alpha}}{m'} + \frac{C_{m_{\dot\theta}}}{I'}\right) + \frac{pC_{n_{\dot\phi}\alpha}}{2\omega_o I'} = \frac{p}{2\omega_o}\left[\frac{1}{2}\frac{I_X}{I}\left(\cdots\right) + \frac{C_{N_{\dot\alpha}}}{I'}\right] \tag{15}$$

$$\Delta\omega = p\left(1 - \frac{I_X}{2I}\right) \qquad = \frac{B}{2} \tag{16}$$

From the new equations for a and b, the following expression can be obtained:

$$\zeta = \zeta_{trim} + R_1 e^{i\nu_{1_e}\left[\lambda_o+\Delta\lambda+i(\omega_o-\Delta\omega)\right]t} + R_2 e^{i\nu_{2_e}\left[\lambda_o-\Delta\lambda-i(\omega_o+\Delta\omega)\right]t}$$

or

$$\zeta = \zeta_{trim} + R_1 e^{(\lambda_o+\Delta\lambda)t_e\, i\left[(\omega_o-\Delta\omega)t+\nu_1\right]} + R_2 e^{(\lambda_o-\Delta\lambda)t_e\, -i\left[(\omega_o+\Delta\omega)t-\nu_2\right]} \tag{17}$$

Inasmuch as a complex number represents a vector which can be expressed in the form $z = a + ib = Re^{i\theta}$, where R represents the magnitude of the vector and θ gives the angular orientation, $R_1e^{(\lambda_o+\Delta\lambda)t}$ and $R_2e^{(\lambda_o-\Delta\lambda)t}$ represent the damping with time of R_1 and R_2, respectively; and $(\omega_o - \Delta\omega)t + \nu_1$ and $(\omega_o + \Delta\omega)t - \nu_2$ give the location of the vectors at any time. These relationships are shown in the following sketch:

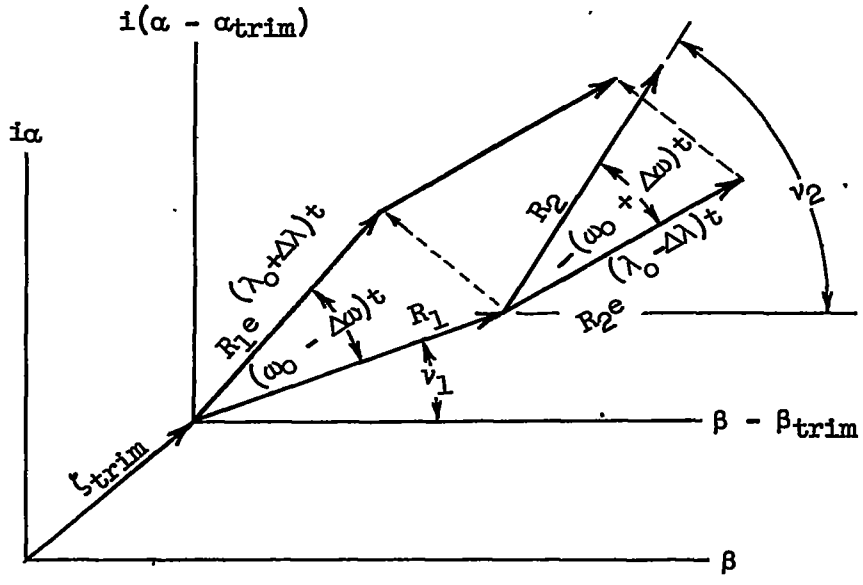

Thus, the resulting motion is given by two damping vectors revolving in different directions and at different rates about the fixed trim.

The time histories of α and β can be obtained from equation (17) by using the relations $e^{i\theta} = \cos\theta + i\sin\theta$ and $\zeta = \beta + i\alpha$; then

$$\begin{aligned}(\beta - \beta_{trim}) + i(\alpha - \alpha_{trim}) = {} & R_1e^{(\lambda_o+\Delta\lambda)t}\cos\left[(\omega_o - \Delta\omega)t + \nu_1\right] + \\ & R_2e^{(\lambda_o-\Delta\lambda)t}\cos\left[(\omega_o + \Delta\omega)t - \nu_2\right] + \\ & i\left\{R_1e^{(\lambda_o+\Delta\lambda)t}\sin\left[(\omega_o - \Delta\omega)t + \nu_1\right] - \right. \\ & \left. R_2e^{(\lambda_o-\Delta\lambda)t}\sin\left[(\omega_o + \Delta\omega)t - \nu_2\right]\right\} \qquad (18)\end{aligned}$$

and

$$\beta - \beta_{trim} = R_1 e^{(\lambda_o+\Delta\lambda)t} \cos\left[(\omega_o - \Delta\omega)t + \nu_1\right] + R_2 e^{(\lambda_o-\Delta\lambda)t} \cos\left[(\omega_o + \Delta\omega)t - \nu_2\right]$$

$$\alpha - \alpha_{trim} = R_1 e^{(\lambda_o+\Delta\lambda)t} \sin\left[(\omega_o - \Delta\omega)t + \nu_1\right] - R_2 e^{(\lambda_o-\Delta\lambda)t} \sin\left[(\omega_o + \Delta\omega)t - \nu_2\right] \tag{19}$$

Thus the oscillation about trim of either α or β is made up of two sinusoidal components which can have different initial magnitudes ($R_1 \neq R_2$) and which can damp at different rates ($\Delta\lambda \neq 0$). When $\Delta\lambda$ approaches the value of λ_o, one of the component oscillations damps rapidly while the other component damps slowly.

Rather than use equations (18) and (19) in the discussion which follows, use will be made of the resultant angle of attack from trim and the angular orientation of this resultant. From equations (18) and (19)

$$\left(\beta - \beta_{trim}\right)^2 + \left(\alpha - \alpha_{trim}\right)^2 = R_1^2 e^{2(\lambda_o+\Delta\lambda)t} + R_2^2 e^{2(\lambda_o-\Delta\lambda)t} + 2R_1R_2e^{2\lambda_o t} \cos\left(2\omega_o t + \nu_1 - \nu_2\right) \tag{20}$$

$$\frac{\alpha - \alpha_{trim}}{\beta - \beta_{trim}} = \frac{R_1 e^{(\lambda_o+\Delta\lambda)t} \sin\left[(\omega_o - \Delta\omega)t + \nu_1\right] - R_2 e^{(\lambda_o-\Delta\lambda)t} \sin\left[(\omega_o + \Delta\omega)t - \nu_2\right]}{R_1 e^{(\lambda_o+\Delta\lambda)t} \cos\left[(\omega_o - \Delta\omega)t + \nu_1\right] + R_2 e^{(\lambda_o-\Delta\lambda)t} \cos\left[(\omega_o + \Delta\omega)t - \nu_2\right]} \tag{21}$$

One interesting point should be made concerning equation (20). The roll rate p appears as an important quantity only in the quantity $\Delta\lambda$, which is small compared with λ_o at low roll rates. Thus, to the first order, a change in the rolling velocity will not influence the resultant oscillation time history, but will only influence the angular orientation

of the resultant. Therefore, the assumption that the rolling velocity is constant may not be too strict a limitation on the validity of the analysis at low roll rates.

The sections which follow discuss the motions of rolling missiles referred to the body-axis system and a technique for reduction of data of missiles employing body-axis instrumentation. In this system forces measured at the center of gravity more conveniently describe the motion than would the angle of attack, which cannot be measured at the center of gravity and must be corrected to the center of gravity.

From the assumption made earlier that aerodynamic forces due to $\dot{\theta}$, $\dot{\psi}$, and $\dot{\phi}$ are negligible, the equations describing the force time histories differ from derived equations only by a constant. If the forces due to $\dot{\theta}$, $\dot{\psi}$, and $\dot{\phi}$ are not negligible, the new equations describing the force time histories differ from equation (17) by the initial conditions R_1, R_2, ν_1, and ν_2.

In the equations and figures to follow, use is made of the symbols as defined in the following table, for either angle-of-attack and sideslip instrumentation or for force-measuring instrumentation. The coefficient C_Z, which is positive downward, has been replaced by $-C_N$.

Symbol	α and β system	C_N and C_Y system
C_R	$\sqrt{(\beta - \beta_{trim})^2 + (\alpha - \alpha_{trim})^2}$	$\sqrt{(C_Y - C_{Y,trim})^2 + (C_N - C_{N,trim})^2}$
$C_{R,trim}$	$\sqrt{\alpha_{trim}^2 + \beta_{trim}^2}$	$\sqrt{(C_{Y,trim} - C_{Y,o})^2 + (C_{N,trim} - C_{N,o})^2}$
Λ	$\tan^{-1} \frac{\alpha - \alpha_{trim}}{\beta - \beta_{trim}}$	$\pi - \tan^{-1} \frac{C_N - C_{N,trim}}{C_Y - C_{Y,trim}}$
Λ_{trim}	$\tan^{-1} \frac{\alpha_{trim}}{\beta_{trim}}$	$\pi - \tan^{-1} \frac{C_{N,trim} - C_{N,o}}{C_{Y,trim} - C_{Y,o}}$

DISCUSSION OF THE DERIVED MOTION

In the discussion to follow, motion is intended to mean the missile motion as reflected by the resultant angle-of-attack or resultant force time histories.

Rolling Trim

By use of the equation $\zeta_{trim} = -C/B$, the rolling trim referenced to the nonrolling trim can be expressed as:

$$\frac{C_{R,trim}}{(C_{R,trim})_{p=0}} = N \frac{1 - \left(\frac{\frac{I_X}{2I}}{1 - \frac{I_X}{2I}}\right)^2 \left(\frac{\Delta\omega}{\omega_o}\right)^2 + \left(\frac{\lambda_o}{\omega_o}\right)^2 \left[1 - \left(\frac{\Delta\lambda}{\lambda_o}\right)^2\right]}{\sqrt{\left[\left(\frac{\lambda_o}{\omega_o}\right)^2 \left(1 - \frac{\Delta\lambda}{\lambda_o}\right)^2 + \left(1 + \frac{\Delta\omega}{\omega_o}\right)^2\right]\left[\left(\frac{\lambda_o}{\omega_o}\right)^2 \left(1 + \frac{\Delta\lambda}{\lambda_o}\right)^2 + \left(1 - \frac{\Delta\omega}{\omega_o}\right)^2\right]}} \tag{22}$$

$$\Lambda_{trim} - (\Lambda_{trim})_{p=0} = \Lambda_N + \tan^{-1} \frac{2\frac{\lambda_o}{\omega_o}\left(\frac{\Delta\lambda}{\lambda_o} + \frac{\Delta\omega}{\omega_o}\right)}{\left(\frac{\lambda_o}{\omega_o}\right)^2 \left[1 - \left(\frac{\Delta\lambda}{\lambda_o}\right)^2\right] + \left[1 - \left(\frac{\Delta\omega}{\omega_o}\right)^2\right]} \tag{23}$$

where

$$N = \sqrt{1 + \frac{4\left(\frac{k}{d}\right)^4 \left(1 - \frac{I_X}{I}\right)^2 \left(\frac{pd}{2V}\right)^2}{\left(\frac{x_o}{d} + \frac{C_{m_q}}{\mu}\right)^2}} \tag{24}$$

$$\Lambda_N = \tan^{-1} - 2\left(\frac{k}{d}\right)^2 \left(1 - \frac{I_X}{I}\right)\frac{pd}{2V} \tag{25}$$

The quantities N and Λ_N are independent of the stability roots λ_o, $\Delta\lambda$, ω_o, and $\Delta\omega$. In addition, N and Λ_N are independent of velocity, and independent of Mach number (if $pd/2V$, C_{m_q}, and x_o/d are constant), and N is influenced slightly by altitude changes (through the C_{m_q}/μ term).

Some examples of rolling-trim magnitude and orientation are given in figures 1 and 2 for a particular missile configuration. The assumed aerodynamic and mass characteristics listed in the figures are representative of a four-fin missile of high fineness ratio. The resonant condition at $\Delta\omega/\omega_o = \pm 1$ is shown in figure 1. An indication of the magnitude of the rolling trim at resonance for low values of damping is also shown. Figure 2 shows that the trim rotates through 180° as the resonance range is passed.

In order to give a better idea of the importance of the resonance range and the associated problem of avoiding resonance, the equations for λ_o/ω_o and $\Delta\omega/\omega_o$ are first written as follows:

$$\frac{\lambda_o}{\omega_o} = \frac{\sqrt{2}\left[1 - \frac{1}{2\left(\frac{k}{d}\right)^2}\frac{C_{m_q}}{C_{N_\alpha}}\right]}{\sqrt{\left[-\frac{2\frac{C_{m_\alpha}}{C_{N_\alpha}}}{\frac{C_{N_\alpha}}{\mu}\left(\frac{k}{d}\right)^2} + \frac{\left(\frac{pd}{2V}\right)^2\left(\frac{I_X}{I}\right)^2}{\left(\frac{C_{N_\alpha}}{\mu}\right)^2} - \left(1 + \frac{1}{2\left(\frac{k}{d}\right)^2}\frac{C_{m_q}}{C_{N_\alpha}}\right)^2\right]\left\{\sqrt{1 + \frac{4\left(\frac{pd}{2V}\right)^2\left[\frac{I_X}{I}\left(1 + \frac{1}{2\left(\frac{k}{d}\right)^2}\frac{C_{m_q}}{C_{N_\alpha}}\right) + \frac{1}{\left(\frac{k}{d}\right)^2}\frac{C_{n_{p_\alpha}}}{C_{N_\alpha}}\right]^2}{\left[-\frac{2\frac{C_{m_\alpha}}{C_{N_\alpha}}}{\frac{C_{N_\alpha}}{\mu}\left(\frac{k}{d}\right)^2} + \frac{\left(\frac{pd}{2V}\right)^2\left(\frac{I_X}{I}\right)^2}{\left(\frac{C_{N_\alpha}}{\mu}\right)^2} - \left(1 + \frac{1}{2\left(\frac{k}{d}\right)^2}\frac{C_{m_q}}{C_{N_\alpha}}\right)^2\right]}} + 1\right\}}} \tag{26}$$

$$\frac{\Delta\omega}{\omega_o} = \frac{2\sqrt{2}\left(\frac{pd}{2V}\right)\left(1 - \frac{I_X}{2I}\right)}{\frac{C_{N_\alpha}}{\mu}\sqrt{\left[-\frac{2\frac{C_{m_\alpha}}{C_{N_\alpha}}}{\frac{C_{N_\alpha}}{\mu}\left(\frac{k}{d}\right)^2} + \frac{\left(\frac{pd}{2V}\right)^2\left(\frac{I_X}{I}\right)^2}{\left(\frac{C_{N_\alpha}}{\mu}\right)^2} - \left(1 + \frac{1}{2\left(\frac{k}{d}\right)^2}\frac{C_{m_q}}{C_{N_\alpha}}\right)^2\right]\left\{\sqrt{1 + \frac{4\left(\frac{pd}{2V}\right)^2\left[\frac{I_X}{I}\left(1 + \frac{1}{2\left(\frac{k}{d}\right)^2}\frac{C_{m_q}}{C_{N_\alpha}}\right) + \frac{1}{\left(\frac{k}{d}\right)^2}\frac{C_{n_{p_\alpha}}}{C_{N_\alpha}}\right]^2}{\left[-\frac{2\frac{C_{m_\alpha}}{C_{N_\alpha}}}{\frac{C_{N_\alpha}}{\mu}\left(\frac{k}{d}\right)^2} + \frac{\left(\frac{pd}{2V}\right)^2\left(\frac{I_X}{I}\right)^2}{\left(\frac{C_{N_\alpha}}{\mu}\right)^2} - \left(1 + \frac{1}{2\left(\frac{k}{d}\right)^2}\frac{C_{m_q}}{C_{N_\alpha}}\right)^2\right]}} + 1\right\}}} \tag{27}$$

Note that both equations (26) and (27) are functions of only the mass characteristics of the missile, the aerodynamic characteristics, and the altitude (through the relative density factor) and are independent of velocity, except indirectly through the effects of Mach number and Reynolds number on the aerodynamic derivatives.

Figure 3 shows the variation of λ_o/ω_o and $\Delta\omega/\omega_o$ with altitude for a high-speed missile. The asymmetries causing the roll were accidental and probably on the order of what can be expected with quality construction of a finned missile. The curves show resonance reached at an altitude of 93,000 feet and at $\lambda_o/\omega_o = -0.022$. Passing through resonance at such a high altitude may be objectionable; for, even though the resultant force may be less than at a lower altitude, the greatly increased trim angle of attack may be such as to put the missile in an unstable angle-of-attack range, which could lead to destruction of the missile or at least to a significant change in flight path. In addition, if the flight path is such that resonance occurs near zenith, then the resonance range will be passed through slowly and large changes in flight path can occur. It may be that, for certain applications, the fins should be deflected, so that resonance occurs at a predetermined low altitude. Although the motion about trim is not greatly affected by changes in rolling velocity at low roll rates, this result does not hold true for the trim if changes in rolling velocity take place near roll resonance.

Motion About Trim

Setting zero time at an oscillation peak ($\nu_1 = \nu_2$) and replacing in equations (20) and (21) the initial conditions R_1, R_2, ν_1, and ν_2 by the following:

$$C_{R,o} = R_1 + R_2$$

$$\Lambda_o = \nu_1 = \nu_2$$

$$K = \frac{R_1 - R_2}{R_1 + R_2}$$

yield the following simplified equations:

$$\left(\frac{C_R}{C_{R,o}}\right)^2 = \frac{e^{2\lambda_o t}}{4}\left[(1 + K)^2 e^{2\Delta\lambda t} + (1 - K)^2 e^{-2\Delta\lambda t} + 2(1 - K^2)\cos 2\omega_o t\right] \quad (28)$$

$$\Lambda = \Lambda_o - \Delta\omega t + \tan^{-1}\frac{(1 + K)e^{\Delta\lambda t} - (1 - K)e^{-\Delta\lambda t}}{(1 + K)e^{\Delta\lambda t} + (1 - K)e^{-\Delta\lambda t}} \tan \omega_o t \qquad (29)$$

A better insight into the physical significance of the quantity K is obtained from the equation for $d\Lambda/dt$:

$$\frac{d\Lambda}{dt} = \frac{\omega_o\left[(1 + K)^2e^{2\Delta\lambda t} - (1 - K)^2e^{-2\Delta\lambda t}\right] + 2(1 - K^2)\Delta\lambda \sin 2\omega_o t}{(1 + K)^2e^{2\Delta\lambda t} + (1 - K)^2e^{-2\Delta\lambda t} + 2(1 - K^2)\cos 2\omega_o t} - \Delta\omega \qquad (30)$$

At $t = 0$

$$\left(\frac{d\Lambda}{dt}\right)_{t=0} = K\omega_o - \Delta\omega \qquad (31)$$

The value of K is thus related to $d\Lambda/dt$ at $t = 0$. Now the motion about trim referred to an axis system in space, which translates, pitches, and yaws with the body-axis system but does not roll, is related to the motion with respect to a body-axis system by the following equations:

$$\left(\frac{C_R}{C_{R,o}}\right)_{space} = \left(\frac{C_R}{C_{R,o}}\right)_{body\ axes}$$

$$\Lambda_{space} = \Lambda_{body\ axes} + pt$$

since the body-axis system rotates at the roll rate p. Thus, the motion in space is determined by the initial conditions Λ_o and $d\Lambda/dt$ at $t = 0$. Also,

$$\left(\frac{d\Lambda_{space}}{dt}\right)_{t=0} = K\omega_o + \frac{1}{2}p\frac{I_X}{I}$$

For values of $\frac{1}{2}p\frac{I_X}{I}$ that are small

$$K = \frac{1}{\omega_o}\left(\frac{d\Lambda_{space}}{dt}\right)_{t=0}$$

Also, for the condition of zero roll rate (p = 0),

$$K = \frac{1}{\omega_0}\left(\frac{d\Lambda_{\text{body axes}}}{dt}\right)_{\substack{t=0\\p=0}} = \frac{1}{\omega_0}\left(\frac{d\Lambda_{\text{space}}}{dt}\right)_{\substack{t=0\\p=0}} = \frac{1}{\omega_0}\left(\frac{d\Lambda_{\text{space}}}{dt}\right)_{\substack{t=0\\ \frac{pI_X}{2I}\to 0}}$$

Thus, from this, the motion from trim in space is nearly independent of the roll rate at low roll rates and low values of I_X/I. Since the motion in space is determined mainly by the value of K, the quantity K is called the "space-motion factor".

Figures 4 and 5 present some typical motions about trim (C_R against Λ with time varied) given by equations (28) and (29) for variable values of K and $\Delta\omega/\omega_0$ and for zero damping (λ_0 and $\Delta\lambda = 0$). The effect of λ_0 on the patterns is mainly to reduce succeeding peaks. The effect of $\Delta\lambda$ is discussed in a subsequent section. The number of cycles to complete the pattern are also shown.

Some of the important characteristics of the motions shown in figures 4 and 5 are as follows:

(1) For $\Delta\omega/\omega_0 = 0$, or for the motion in space, the pattern is elliptical, varying from a line (motion in one plane) for $K = 0$ to a circle for $K = \pm 1$.

(2) Whether K is positive or negative can be easily detected, for C_R circles the trim center for negative values of K, but does not for positive values of K.

(3) An indication of the approach of resonance is shown by the tendency for the loops to close on each other and become coincident for a given value of K.

(4) Whether the missile is above or below roll resonance is immediately determined, since the motion above resonance is characterized by inside loops, and the motion below roll resonance by outside loops.

(5) In order to determine the value of the rolling trim from a plot of C_N against C_Y, a low value of K is desirable.

As indicated, a plot of C_N against C_Y (or C_R against Λ) will yield immediately valuable information about the motion.

Rolling influences the damped motion through the term $\Delta\lambda$. From equation (28) the envelopes of C_R are:

$$\frac{C_{R,max}}{C_{R,o}} = \frac{e^{\lambda_o t}}{2}\left[(1 + K)e^{\Delta\lambda t} + (1 - K)e^{-\Delta\lambda t}\right] \tag{32}$$

$$\frac{C_{R,min}}{C_{R,o}} = \frac{e^{\lambda_o t}}{2}\left[(1 + K)e^{\Delta\lambda t} - (1 - K)e^{-\Delta\lambda t}\right] \tag{33}$$

Typical oscillation envelopes of C_R below divergence ($\Delta\lambda < \lambda_o$) are shown in figure 6. The figure shows that the effect of an increase in $\Delta\lambda$ tends to damp the oscillation of C_R more highly, except for positive values of K. For positive values of K the oscillation becomes less damped with an increase in $\Delta\lambda/\lambda_o$, up to the time where $C_{R,min} = 0$. But with further increases in time, the oscillation becomes highly damped. Whether $\Delta\lambda/\lambda_o$ is positive or negative can be obtained from the following equation for $\Delta\lambda/\lambda_o$:

$$\frac{\Delta\lambda}{\lambda_o} = -\frac{\frac{I_X}{2I}\left(C_{N_\alpha} + \frac{1}{2\left(\frac{k}{d}\right)^2}C_{m_q}\right)}{1 - \frac{I_X}{2I}\left(C_{N_\alpha} - \frac{1}{2\left(\frac{k}{d}\right)^2}C_{m_q}\right)}\frac{\Delta\omega}{\omega_o} - \frac{1}{1 - \frac{I_X}{2I}}\frac{\frac{1}{2\left(\frac{k}{d}\right)^2}C_{n_{p_\alpha}}}{\left(C_{N_\alpha} - \frac{1}{2\left(\frac{k}{d}\right)^2}C_{m_q}\right)}\frac{\Delta\omega}{\omega_o} \tag{34}$$

For conventional missile configurations $\frac{1}{2\left(\frac{k}{d}\right)^2}C_{m_q}$ is negative and of greater magnitude than C_{N_α}; as a result $\Delta\lambda/\lambda_o$ usually has the same sign as $\Delta\omega/\omega_o$.

Since the limiting magnitude of $\Delta\omega/\omega_o$ is $\frac{1 - \frac{I_X}{2I}}{\frac{I_X}{2I}}$ and $\frac{C_{N_\alpha} + \frac{1}{2\left(\frac{k}{d}\right)^2}C_{m_q}}{C_{N_\alpha} - \frac{1}{2\left(\frac{k}{d}\right)^2}C_{m_q}}$ can be between ± 1, $\Delta\lambda/\lambda_o$ will never exceed ± 1, if

$C_{n_{p\alpha}}$ is negative. However, a positive value of $C_{n_{p\alpha}}$ can lead to instability at high roll rates or high altitudes, or both. However, the instability resulting from a positive $C_{n_{p\alpha}}$ will be serious only if it occurs at altitudes where significant dynamic pressure exists, since the rate of divergence is negligible at extremely high altitudes. Thus, knowledge of the value of $C_{n_{p\alpha}}$ is most important for missiles which roll rapidly.

Another way of visualizing the effect of $\Delta\lambda$ on the motion is obtained by finding the variation of K from peak to peak of the oscillations or effectively setting the initial conditions and zero time at succeeding peaks. Then, from equations (30) and (31),

$$K_t = \frac{(1 + K)e^{\Delta\lambda t} - (1 - K)e^{-\Delta\lambda t}}{(1 + K)e^{\Delta\lambda t} + (1 - K)e^{-\Delta\lambda t}}$$

Since $e^{\Delta\lambda t}$ or $e^{-\Delta\lambda t} \rightarrow 0$ as $t \rightarrow \infty$, $K_t \rightarrow \pm 1$ as $t \rightarrow \infty$. Thus, $\Delta\lambda$ causes the motion to tend toward that given by $K = \pm 1$ in figure 5. Figure 6 is in agreement with this concept. Of course, at low roll rates this trend is completely obscured since the oscillation is, for all practical purposes, damped out by the time the influence of $\Delta\lambda$ is felt.

RESPONSE OF ROLLING MISSILES TO FORCING FUNCTIONS

Thus far, motions resulting from variable initial conditions have been discussed. Remaining to be determined are the initial conditions (and as a result the motions) that can be expected from given disturbances.

Response to a Trim Change

Assume that, at the time of the instantaneous control deflection, the missile was at the initial trim and the oscillation about this initial trim had completely damped out. The initial conditions are referred to an axis system at $\alpha - \alpha_{trim}$, $\beta - \beta_{trim}$ about which the oscillation takes place,

as indicated on the following sketch:

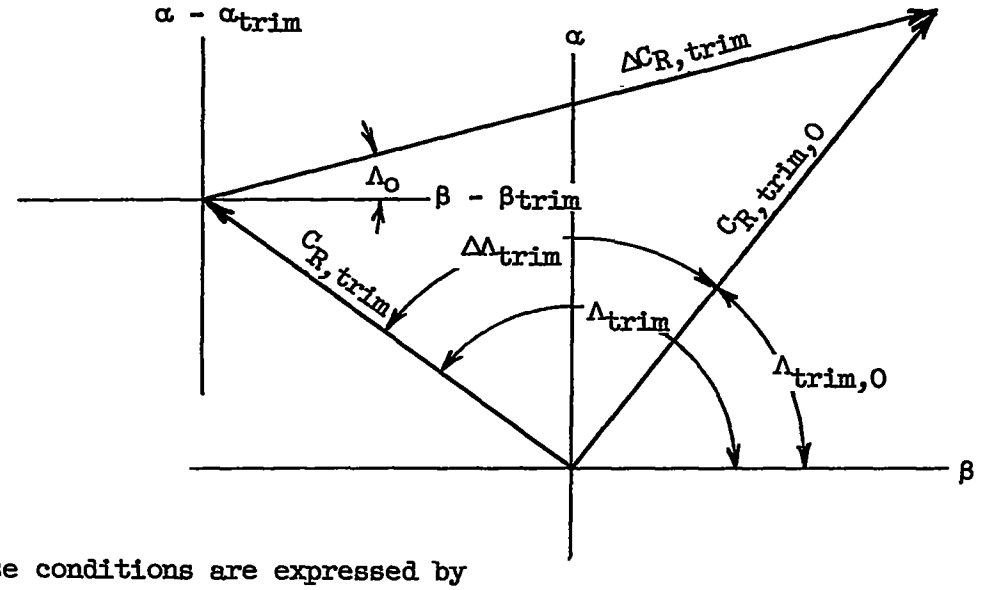

These conditions are expressed by

$$\left(\zeta - \zeta_{trim}\right)_{t=0} = \Delta C_{R,trim} e^{i\Lambda_o}$$

$$\dot{\zeta}_{t=0} = 0$$

where

$$\Delta C_{R,trim} = \sqrt{\left(C_{R,trim}\right)^2 + \left(C_{R,trim}\right)_o^2 - 2C_{R,trim}\left(C_{R,trim}\right)_o \cos \Delta\Lambda_{trim}}$$

and

$$\Lambda_o = \tan^{-1} \frac{\left(C_{R,trim}\right)_o \sin \Lambda_{trim,o} - C_{R,trim} \sin \Lambda_{trim}}{\left(C_{R,trim}\right)_o \cos \Lambda_{trim,o} - C_{R,trim} \cos \Lambda_{trim}}$$

Substituting these initial conditions into equation (17) gives the following values for R_1, R_2, and $\nu_2 - \nu_1$:

$$\frac{R_1}{\Delta C_{R,trim}} = \frac{\sqrt{(\omega_o + \Delta\omega)^2 + (\lambda_o - \Delta\lambda)^2}}{2\sqrt{\omega_o^2 + \Delta\lambda^2}}$$

$$\frac{R_2}{\Delta C_{R,trim}} = \frac{\sqrt{(\omega_o - \Delta\omega)^2 + (\lambda_o + \Delta\lambda)^2}}{2\sqrt{\omega_o^2 + \Delta\lambda^2}}$$

$$\nu_2 - \nu_1 = \pi - \tan^{-1}\frac{(\omega_o - \Delta\omega)}{-(\lambda_o + \Delta\lambda)} - \tan^{-1}\frac{(\omega_o + \Delta\omega)}{-(\lambda_o - \Delta\lambda)}$$

Neglecting $\Delta\lambda$ gives as the maximum value of C_R, from equation (20),

$$C_{R,max} = e^{\lambda_o t^*}(R_1 + R_2)$$

at the time t^*, which is given by

$$t^* = \frac{\nu_2 - \nu_1}{2\omega_o}$$

Assume that λ_o and $\Delta\lambda$ are small quantities compared with ω_o and $\Delta\omega$. For $\Delta\omega < \omega_o$,

$$t^* = 0$$

$$C_{R,max} = \Delta C_{R,trim}$$

For $\Delta\omega > \omega_o$,

$$t^* = \frac{\pi}{2\omega_o}$$

$$C_{R,max} = \frac{\Delta\omega}{\omega_o} \Delta C_{R,trim} e^{\pi\lambda_o/2\omega_o}$$

The value for K is

$$K = \frac{R_1 - R_2}{R_1 + R_2}$$

Then, for $\Delta\omega < \omega_o$

$$K = \frac{\Delta\omega}{\omega_o}$$

and for $\Delta\omega > \omega_o$

$$K = \frac{1}{\Delta\omega/\omega_o}$$

These results are plotted in figure 7. It should not be inferred from figure 7 that the value of $C_{R,max}$ increases with an increase in $\Delta\omega/\omega_o$ above $\Delta\omega/\omega_o = 1$, since $C_{R,max}$ is referenced to $\Delta C_{R,trim}$, which drops off rapidly with an increase in $\Delta\omega/\omega_o$ above $\Delta\omega/\omega_o = 1$, as is shown in figure 1. Note that, since the space-motion factor K and $\Delta\omega/\omega_o$ are of the same sign, only the motion patterns for positive values of K in figures 4 and 5 are possible.

Response to Pulse-Rocket Disturbance

A free-flight missile can be conveniently disturbed from its equilibrium conditions by firing a small rocket charge mounted normal to the longitudinal axis and forward or rearward of the center of gravity. Such a rocket charge is referred to as a "pulse rocket." For this simplified analysis the rocket thrust is assumed to be constant. However the pulse-rocket total impulse (area under the curve of thrust plotted against time) and the pulse-rocket burning time, rather than pulse-rocket thrust, are used as variables. By use of methods similar to those used in the section "Development of Equations of Motion", solutions have been obtained for the peak value of C_R and the value of K at the peak, for cases where the peak C_R occurs before rocket burnout and after rocket burnout. The

results are presented in figures 8 and 9 for the special case of zero damping ($\lambda_o = 0$, $\Delta\lambda = 0$).

Figure 8 shows the large effect the roll rate can have on the peak value of C_R, where C_R is indicative of the resultant angle of attack. Figure 9 shows that the space-motion factor K rapidly approaches 1 at a given pulse-rocket burning time, as $\Delta\omega/\omega_o$ increases in magnitude. Both figures show the desirability of a very low pulse-rocket burning time, first in order to obtain a high peak C_R occurring after pulse-rocket burnout, and second in order to restrict the motion to nearly one plane in space.

APPLICATION OF EQUATIONS OF MOTION TO ESTABLISHMENT OF A TECHNIQUE FOR REDUCTION OF OSCILLATION DATA

The procedure used in applying the equations of motion for the purpose of reducing the oscillation data is presented in two parts. The first part deals with the determination of the stability roots, λ_o, $\Delta\lambda$, ω_o, and $\Delta\omega$, and the second part deals with a method for obtaining the static and dynamic aerodynamic derivatives from the stability roots. It is shown that the derivatives can be found by measuring four quantities in addition to airspeed and atmospheric conditions. Of course, the accuracy of the derivatives obtained depends, to a large extent, on how well the assumptions set down in the previous analysis are satisfied.

Determination of Stability Roots

Consider a rolling missile employing instrumentation at the center of gravity for measuring the normal-force and side-force coefficients. If the missile is disturbed in such a manner that the space-motion factor K is near zero and is out of the region of roll resonance so that the trim does not wander in magnitude and direction, plots of C_N against C_Y (or C_R against Λ) similar to those shown in figure 4 and 5 can be obtained. A typical experimental plot is shown in figure 10. With the low values of K, a fairly reliable trim center can be assumed.

The quantity $\Delta\omega/\omega_o$ is readily found by measuring the angle between adjacent peaks on the plot of C_N against C_Y. (See following sketch.)

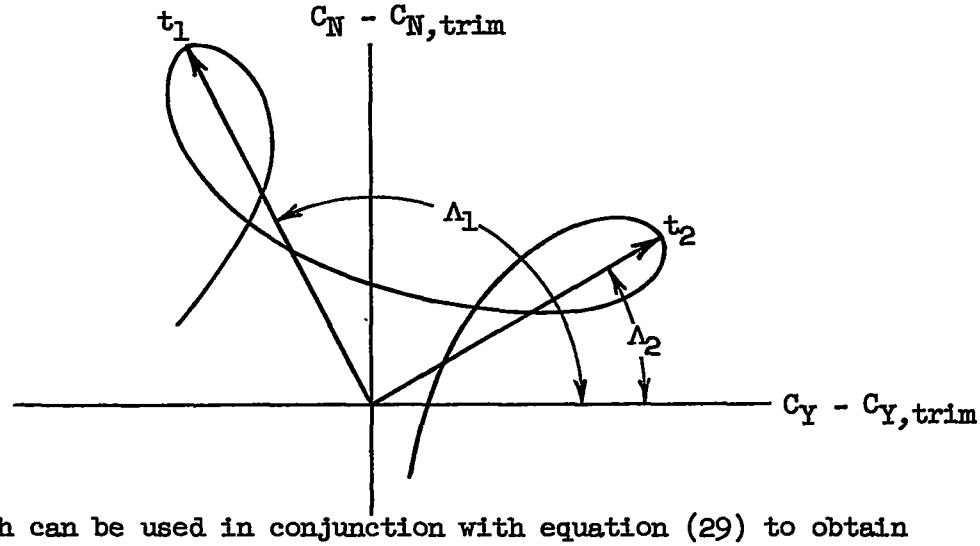

This sketch can be used in conjunction with equation (29) to obtain

$$\Lambda_1 = \Lambda_o - \Delta\omega t_1$$

$$\Lambda_2 = \Lambda_o - \Delta\omega t_2 + \pi$$

$$\Lambda_2 - \Lambda_1 = -\Delta\omega(t_2 - t_1) + \pi$$

and since t_2 and t_1 are measured at adjacent oscillation peaks

$$t_2 - t_1 = \frac{\pi}{\omega_o}$$

and

$$\frac{\Delta\omega}{\omega_o} = 1 - \frac{\Lambda_2 - \Lambda_1}{\pi} \tag{35}$$

Calculation of $\Delta\omega/\omega_o$ for all adjacent oscillation peaks gives an indication of the validity of the assumption that the roll rate p is constant. Also the accuracy of the calculated $\Delta\omega$ is affected by the correctness of

the assumed trim. The following table presents the calculated values of $\Delta\omega/\omega_o$ for the experimental plot of figure 10:

Peaks	$\Delta\omega/\omega_o$
1 to 2	0.301
2 to 3	.325
3 to 4	.282
4 to 5	.308

The small variation of $\Delta\omega/\omega_o$ upholds the assumption of a nearly constant roll rate.

With the trim center known, the time history of C_R^2 can be obtained from the plot of C_N against C_Y. If sufficient oscillations are present, the damping envelopes about the oscillation peaks can be drawn with good accuracy. Equations (32) and (33) represent the time histories of the damping envelopes. If use is made of the damping envelopes, equation (28) can be written as:

$$C_R^2 = \frac{1}{2}\left[\left(C_{R,max}\right)^2 + \left(C_{R,min}\right)^2\right] + C_{R,o}^2(1 - K^2)e^{2\lambda_o t}\cos 2\omega_o t \qquad (36)$$

Thus from this equation, C_R^2 is a sinusoidal damped oscillation about a trim given by $\frac{1}{2}\left[\left(C_{R,max}\right)^2 + \left(C_{R,min}\right)^2\right]$. From the period of oscillation ω_o can be obtained. From equations (32) and (33) and the damping envelopes,

$$\frac{1}{2}\log\left[\left(C_{R,max}\right)^2 - \left(C_{R,min}\right)^2\right] = \lambda_o t + \text{Constant} \qquad (37)$$

$$\frac{1}{2}\log\left(\frac{C_{R,max} + C_{R,min}}{C_{R,max} - C_{R,min}}\right) = \Delta\lambda t + \text{Constant} \qquad (38)$$

Thus, λ_o and $\Delta\lambda$ are obtained from the slopes of plots of $\frac{1}{2}\log\left[\left(C_{R,max}\right)^2 - \left(C_{R,min}\right)^2\right]$ and $\frac{1}{2}\log\left(\frac{C_{R,max} + C_{R,min}}{C_{R,max} - C_{R,min}}\right)$ against time.

Figure 11 is a plot of C_R^2 obtained from figure 10. Except near the end of the oscillation, where an error in the assumed trim would have a large effect on time for the oscillation peak, the periods measured at oscillation peaks appear quite good. If an average period of 0.280 second is used,

$$\omega_o = \frac{\pi}{0.280} = 11.20$$

Two special corrections were also used in evaluating the damping λ_o. First, since the assumed trim may not be correct, the error would appear as an oscillation in $\frac{1}{2}\left[\left(C_{R,max}\right)^2 + \left(C_{R,min}\right)^2\right]$. As a result, the periods measured at points where the oscillation cuts $\frac{1}{2}\left[\left(C_{R,max}\right)^2 + \left(C_{R,min}\right)^2\right]$ would be inconsistent and differ from the periods measured at the peaks. An indication of the trim error is given by this inconsistency of the period. As a result an adjusted value of $\frac{1}{2}\left[\left(C_{R,max}\right)^2 + \left(C_{R,min}\right)^2\right]$ has been determined for each half cycle, such that the period is consistent with the adjacent peak periods. These adjustments to $\frac{1}{2}\left[\left(C_{R,max}\right)^2 + \left(C_{R,min}\right)^2\right]$ are indicated by the dashed lines. While this correction is admittedly crude, it will provide a more nearly correct damping curve.

The second correction is in consequence of the high speed and the flight path of this particular model. As a result, the air-density change during this plotted oscillation was significant. On the assumption that the change in air density does not force the model oscillation, the damping at any time during the oscillation (if the velocity change is assumed negligible) can be written as

$$\lambda_{o,t} = \lambda_{o,t=0}\left(\frac{\rho}{\rho_{t=0}}\right)$$

Then from equation (37)

$$\frac{1}{2}\log\left[\left(C_{R,max}\right)^2 - \left(C_{R,min}\right)^2\right] = \lambda_{o,t=0}\left(\frac{t\rho}{\rho_{t=0}}\right)$$

Thus, this correction appears as a time adjustment. Figure 12 presents the damping determined, including the effects of each correction. From the slope of the lower plot in figure 12,

$$\lambda_o = -0.736$$

Because of the low roll rate, $\Delta\lambda$ is small and cannot be obtained from figure 11, since $(C_{R,min})^2 \approx 0$.

Determination of Aerodynamic Derivatives From Stability Roots

First, equations are written for the differential accelerations at two points on the missile as measured by normal and transverse accelerometers:

$$\Delta a_Z = a_Z(x_2,y_2,z_2) - a_Z(x_1,y_1,z_1)$$

$$= -(x_2 - x_1)\left[\sum \frac{M_Y}{I} - \frac{I_X}{I}\dot{\phi}\dot{\psi}\right] - (z_2 - z_1)\dot{\phi}^2$$

$$\Delta a_Y = a_Y(x_2,y_2,z_2) - a_Y(x_1,y_1,z_1)$$

$$= (x_2 - x_1)\left[\sum \frac{M_Z}{I} + \frac{I_X}{I}\dot{\phi}\dot{\theta}\right] - (y_2 - y_1)\dot{\phi}^2$$

These equations were derived under the same assumptions that were made in the section "Development of Equations of Motion". Since $\Delta C_N = -m\Delta a_Z/qA_F$ and $\Delta C_Y = m\Delta a_Y/qA_F$,

$$\Delta C_N = \frac{md(x_2 - x_1)}{I}\left[\sum \frac{M_Y}{qA_F d} - I'\dot{\phi}\frac{I_X}{I}\dot{\psi}\right] + \frac{m(z_2 - z_1)\dot{\phi}^2}{qA_F}$$

and

$$\Delta C_Y = \frac{md(x_2 - x_1)}{I}\left[\sum \frac{M_Z}{qA_F d} + I'\dot{\phi}\frac{I_X}{I}\dot{\theta}\right] - \frac{m(y_2 - y_1)\dot{\phi}^2}{qA_F}$$

By use of equations (1) and (2),

$$\dot{\psi} = \frac{C_Y}{m'} - \dot{\beta} + \dot{\phi}\alpha$$

$$\dot{\theta} = \frac{C_N}{m'} + \dot{\alpha} + \dot{\phi}\beta$$

If, then,

$$C_N = C_{N_\alpha}\alpha + C_{N,o} \qquad \alpha = \frac{C_N - C_{N,o}}{C_{N_\alpha}} \qquad \dot{\alpha} = \frac{\dot{C}_N}{C_{N_\alpha}}$$

$$C_Y = C_{N_\alpha}\beta + C_{Y,o} \qquad \beta = -\frac{(C_Y - C_{Y,o})}{C_{N_\alpha}} \qquad \dot{\beta} = -\frac{\dot{C}_Y}{C_{N_\alpha}}$$

and

$$\sum \frac{M_Y}{qA_F d} = C_{m_\alpha}\alpha + C_{n_{p_\alpha}}\frac{pd}{2V}\beta + C_{m_q}\frac{\dot{\theta}d}{2V} + C_{N,o}\frac{x_o}{d}$$

$$\sum \frac{M_Z}{qA_F d} = -C_{m_\alpha}\beta + C_{n_{p_\alpha}}\frac{pd}{2V}\alpha + C_{m_q}\frac{\dot{\psi}d}{2V} - C_{Y,o}\frac{x_o}{d}$$

Then,

$$\Delta C_N = \frac{1}{\left(\frac{k}{d}\right)^2}\left(\frac{x_2}{d} - \frac{x_1}{d}\right)\left[\frac{C_{m_\alpha}}{C_{N_\alpha}} + \frac{C_{m_q}}{\mu} - \frac{2}{C_{N_\alpha}}\mu\left(\frac{pd}{2V}\right)^2\left(\frac{k}{d}\right)^2\frac{I_X}{I}\right]C_N +$$

$$\text{Constant} + \frac{1}{\left(\frac{k}{d}\right)^2}\left(\frac{x_2}{d} - \frac{x_1}{d}\right)\left\{\frac{C_{m_q}}{C_{N_\alpha}}\frac{\dot{C}_N d}{2V} - \frac{pd}{2V}\left[\left(\frac{C_{n_{p_\alpha}}}{C_{N_\alpha}}\frac{C_{m_q}}{C_{N_\alpha}} + 2\left(\frac{k}{d}\right)^2\frac{I_X}{I}\right)C_Y + \frac{2}{C_{N_\alpha}}\mu\left(\frac{k}{d}\right)^2\frac{I_X}{I}\frac{\dot{C}_Y d}{2V}\right]\right\} \tag{39}$$

$$\Delta C_Y = \frac{1}{\left(\frac{k}{d}\right)^2}\left(\frac{x_2}{d} - \frac{x_1}{d}\right)\left[\frac{C_{m_\alpha}}{C_{N_\alpha}} + \frac{C_{m_q}}{\mu} - \frac{2}{C_{N_\alpha}}\mu\left(\frac{pd}{2V}\right)^2\left(\frac{k}{d}\right)^2\frac{I_X}{I}\right]C_Y +$$

$$\text{Constant} + \frac{1}{\left(\frac{k}{d}\right)^2}\left(\frac{x_2}{d} - \frac{x_1}{d}\right)\left\{\frac{C_{m_q}}{C_{N_\alpha}}\frac{\dot{C}_Y d}{2V} + \frac{pd}{2V}\left[\left(\frac{C_{n_{p_\alpha}}}{C_{N_\alpha}} + \frac{C_{m_q}}{C_{N_\alpha}} + 2\left(\frac{k}{d}\right)^2\frac{I_X}{I}\right)C_N + \frac{2}{C_{N_\alpha}}\mu\left(\frac{k}{d}\right)^2\frac{I_X}{I}\frac{\dot{C}_N d}{2V}\right]\right\} \tag{40}$$

The last bracketed terms of equations (39) and (40) represent the corrections that must be made to ΔC_N and ΔC_Y in order to obtain linear plots of C_N against C_Y. Note that the influence of the roll can make the correction large even for low roll rates and small ratios of I_X to I. At high roll rates the correction may become greater than the quantity to be determined. Figures 13 and 14 present experimental plots of ΔC_N against C_N and ΔC_Y against C_Y. However, for simplicity the points were taken near the oscillation peaks (ΔC_N points near $C_{N_{peak}}$, ΔC_Y points near $C_{Y_{peak}}$) where $\dot{C}_N$ and $\dot{C}_Y$ are negligible. Thus any corrections that must be made to the upper plots of figures 13 and 14 result entirely from the roll effect on ΔC_N and ΔC_Y. The effect of rolling on curves of ΔC_Y against C_Y (upper plot, fig. 13) makes the curve appear nonlinear, whereas the effect on ΔC_N plotted against C_N (upper plot, fig. 14) appears as an increase in scatter. The correction for roll given in the preceding equations by use of estimated derivatives

reduces the scatter and removes the nonlinearities, as shown in the lower plots of figures 13 and 14. The differences of 10 percent in slopes as obtained in the C_N and C_Y planes is not understood. The effect may be real, resulting from different aeroelastic effects on the fins of the model, or be within the accuracy of the data.

The slope s of the curve of ΔC_N plotted against C_N and ΔC_Y against C_Y is related to ω_o, $\Delta\omega$, λ_o, and $\Delta\lambda$ by the equation:

$$s = \frac{1}{\left(\frac{k}{d}\right)^2}\left(\frac{x_2}{d} - \frac{x_1}{d}\right)\left[\frac{C_{m_\alpha}}{C_{N_\alpha}} + \frac{C_{m_q}}{\mu} - \frac{2\mu}{C_{N_\alpha}}\left(\frac{pd}{2V}\right)^2\left(\frac{k}{d}\right)^2\frac{I_X}{I}\right]$$

$$= -\frac{2\mu}{C_{N_\alpha}}\left(\frac{d}{2V}\right)^2\left(\frac{x_2}{d} - \frac{x_1}{d}\right)\left[\omega_o^2 + \lambda_o^2 - \Delta\lambda^2 + \frac{\frac{I_X}{I}\left(1 - \frac{I_X}{4I}\right)}{\left(1 - \frac{I_X}{2I}\right)^2}\Delta\omega^2\right] \quad (41)$$

Thus,

$$C_{N_\alpha} = \frac{-2\mu\left(\frac{x_2}{d} - \frac{x_1}{d}\right)\left(\frac{d}{2V}\right)^2}{s}\left[\omega_o^2 + \lambda_o^2 - \Delta\lambda^2 + \Delta\omega^2\frac{\frac{I_X}{I}\left(1 - \frac{I_X}{4I}\right)}{\left(1 - \frac{I_X}{2I}\right)^2}\right] \quad (42)$$

For the test model, the necessary constants are:

$$\mu = 76{,}600$$

$$\frac{2V}{d} = 8{,}120$$

$$\frac{k}{d} = 2.60$$

$$\frac{I_X}{I} = 0.027$$

$$\frac{x_2}{d} - \frac{x_1}{d} = -2.94$$

Then using the average of slopes from figures 13 and 14 gives

$$C_{N_\alpha} = 0.0344\left(125.5 + 0.54 + 0.34\right) = 4.35$$

From equation (13)

$$C_{m_q} = 2\left(\frac{k}{d}\right)^2\left(\frac{2\mu d}{2V}\lambda_o + C_{N_\alpha}\right) \tag{43}$$

Then

$$C_{m_q} = 13.5\left[\frac{2(76600)}{8120}(-0.736) + 4.35\right]$$

$$C_{m_q} = 13.5(-13.90 + 4.35) = -129$$

Equation (41) can be rewritten as:

$$C_{m_\alpha} = -2\left(\frac{k}{d}\right)^2\mu\left(\frac{d}{2V}\right)^2\left[\omega_o^2 + \lambda_o^2 - \Delta\lambda^2 - \frac{\left(\frac{I_X}{2I}\right)^2}{\left(1 - \frac{I_X}{2I}\right)^2}\Delta\omega^2\right] - \frac{C_{N_\alpha}C_{m_q}}{\mu} \tag{44}$$

Then

$$C_{m_\alpha} = -0.0156(125.5 + 0.54 - 0.0023) - 0.00732$$

$$= -1.97 - 0.007 = -1.977$$

and

$$\frac{dC_m}{dC_N} = \frac{C_{m_\alpha}}{C_{N_\alpha}} = -\frac{1.977}{4.35} = -0.455$$

With C_{N_α} and C_{m_q} known, the derivative $C_{n_{p_\alpha}}$ can be obtained from equation (34) and is given by:

$$C_{n_{p_\alpha}} = -\frac{2\left(\frac{k}{d}\right)^2\left(1 - \frac{I_X}{2I}\right)\left(C_{N_\alpha} - \frac{1}{2\left(\frac{k}{d}\right)^2} C_{m_q}\right)\Delta\lambda\omega_o}{\Delta\omega\lambda_o} - \frac{\left(\frac{k}{d}\right)^2 \frac{I_X}{I}\left(C_{N_\alpha} + \frac{1}{2\left(\frac{k}{d}\right)^2} C_{m_q}\right)}{4} \tag{45}$$

A value of $C_{n_{p_\alpha}}$ for the test model could not be determined, since $\Delta\lambda$ could not be determined with any accuracy at the low roll rates of the test.

It should be emphasized that the biggest drawback in obtaining good accuracy is in failure to determine the trim center correctly. In order to obtain a reliable trim center, the missile should be disturbed in such manner that K is small in magnitude, and the resonance range should be avoided.

CONCLUDING REMARKS

An analysis has been made of the motions of rolling missiles having slight aerodynamic asymmetries. The motions were referred to a body axis system. The type of motion encountered by the missile is shown to be dependent on the ratio of the rolling velocity to pitching frequency and the manner in which the missile is disturbed. The equations of motion were found to be useful in establishing a technique for the reduction of oscillation data for rolling missiles having body-axis instrumentation. The method was applied to experimental results obtained from flight tests of a rolling missile configuration.

Langley Aeronautical Laboratory,
National Advisory Committee for Aeronautics.
Langley Field, Va., May 1, 1956.

REFERENCES

1. Jones, B. Melvill: Dynamics of the Aeroplane. Vol. V of Aerodynamic Theory, div. N; W.F. Durand, ed., Julius Springer (Berlin), 1935, pp. 1-222.

2. Fowler, R. H., Gallop, E. G., Lock, C. N. H., and Richmond, H. W.: The Aerodynamics of a Spinning Shell. Phil. Trans. Roy. Soc. (London), ser. A, vol. 221, 1920, pp. 295-387.

3. Nicolaides, John D.: On The Free Flight Motion of Missiles Having Slight Configurational Asymmetries. Rep. No. 858, Ballistic Res. Labs., Aberdeen Proving Ground, June 1953.

4. Charters, A. C.: The Linearized Equations of Motions Underlying the Dynamic Stability of Aircraft, Spinning Projectiles, and Symmetrical Missiles. NACA TN 3350, 1955.

5. Phillips, William H.: Effect of Steady Rolling on Longitudinal and Directional Stability. NACA TN 1627, 1948.

6. Bolz, Ray E.: Dynamic Stability of a Missile in Rolling Flight. Jour. Aero. Sci., vol. 19, no. 6, June 1952, pp. 395-403.

7. Mitcham, Grady L., Stevens, Joseph E., and Norris, Harry P.: Aerodynamic Characteristics and Flying Qualities of a Tailless Triangular-Wing Airplane Configuration As Obtained From Flights of Rocket-Propelled Models at Transonic and Low Supersonic Speeds. NACA RM L9L07, 1950.

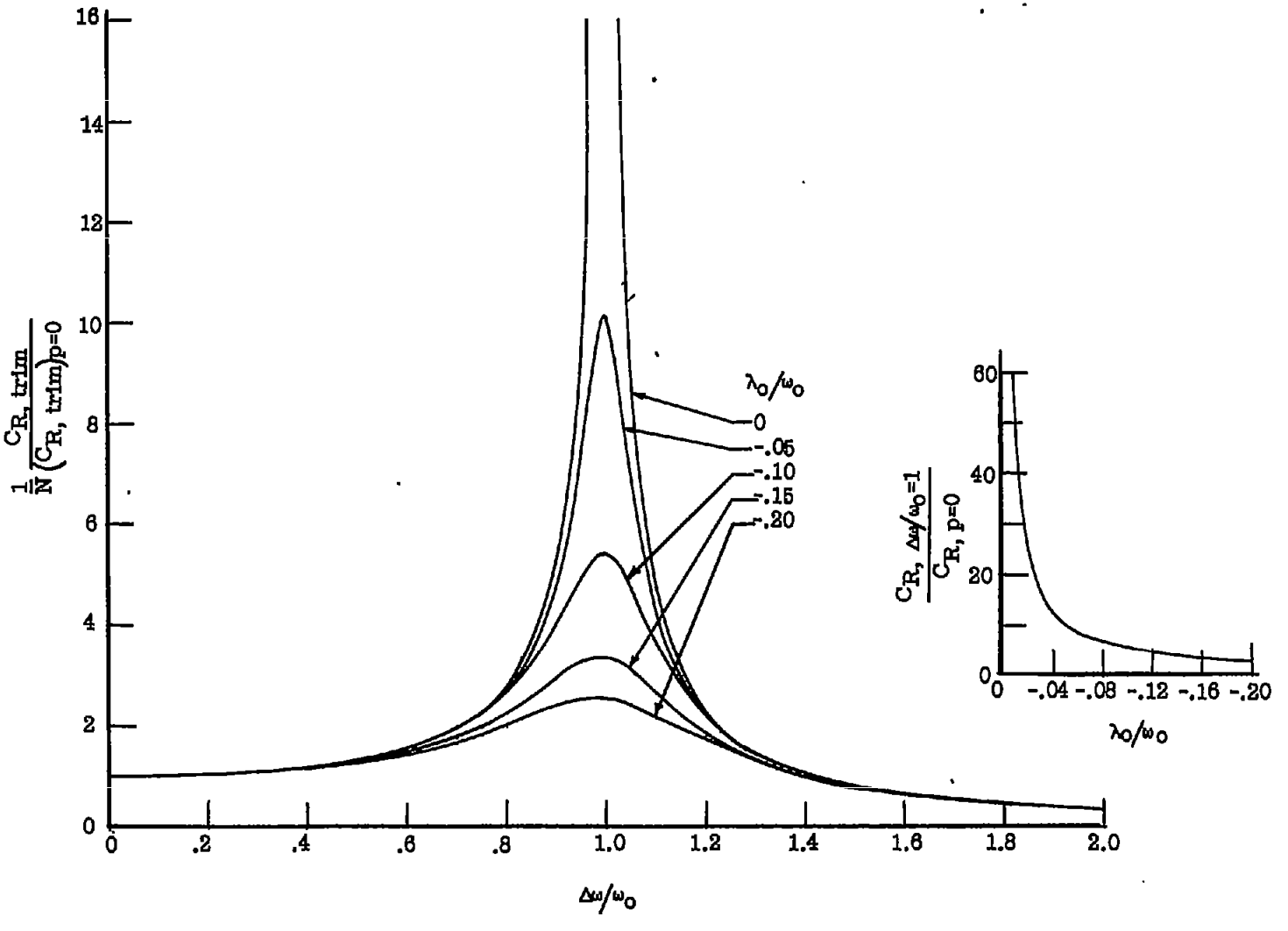

Figure 1.- Examples of rolling trim magnitude for a particular missile configuration. The quantity N is defined by equation (24). $\frac{I_X}{I} = 0.0392$; $\frac{1}{2(k/d)^2}\frac{C_{m_q}}{C_{N_\alpha}} = -3$; $C_{n_{p\alpha}} = 0$.

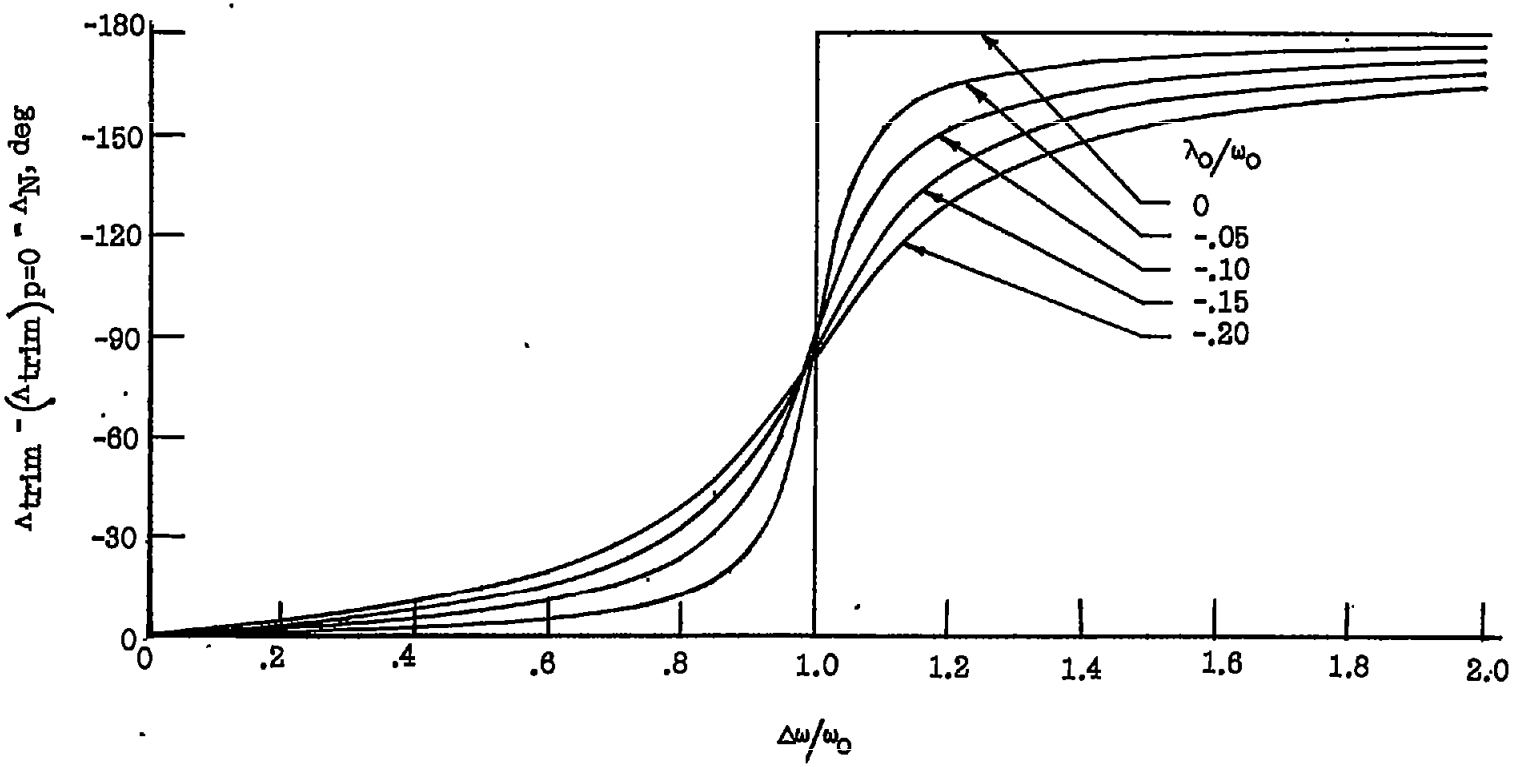

Figure 2.- Angular orientation of rolling trim for a particular missile. $\frac{I_X}{I} = 0.0392$; $\frac{1}{2(k/d)^2}\frac{C_{m_q}}{C_{N_\alpha}} = -3$; $C_{n_{p\alpha}} = 0$. The angle Λ_N is defined by equation (25). (For negative values of $\Delta\omega/\omega_o$, the sign of Λ_{trim} is reversed.)

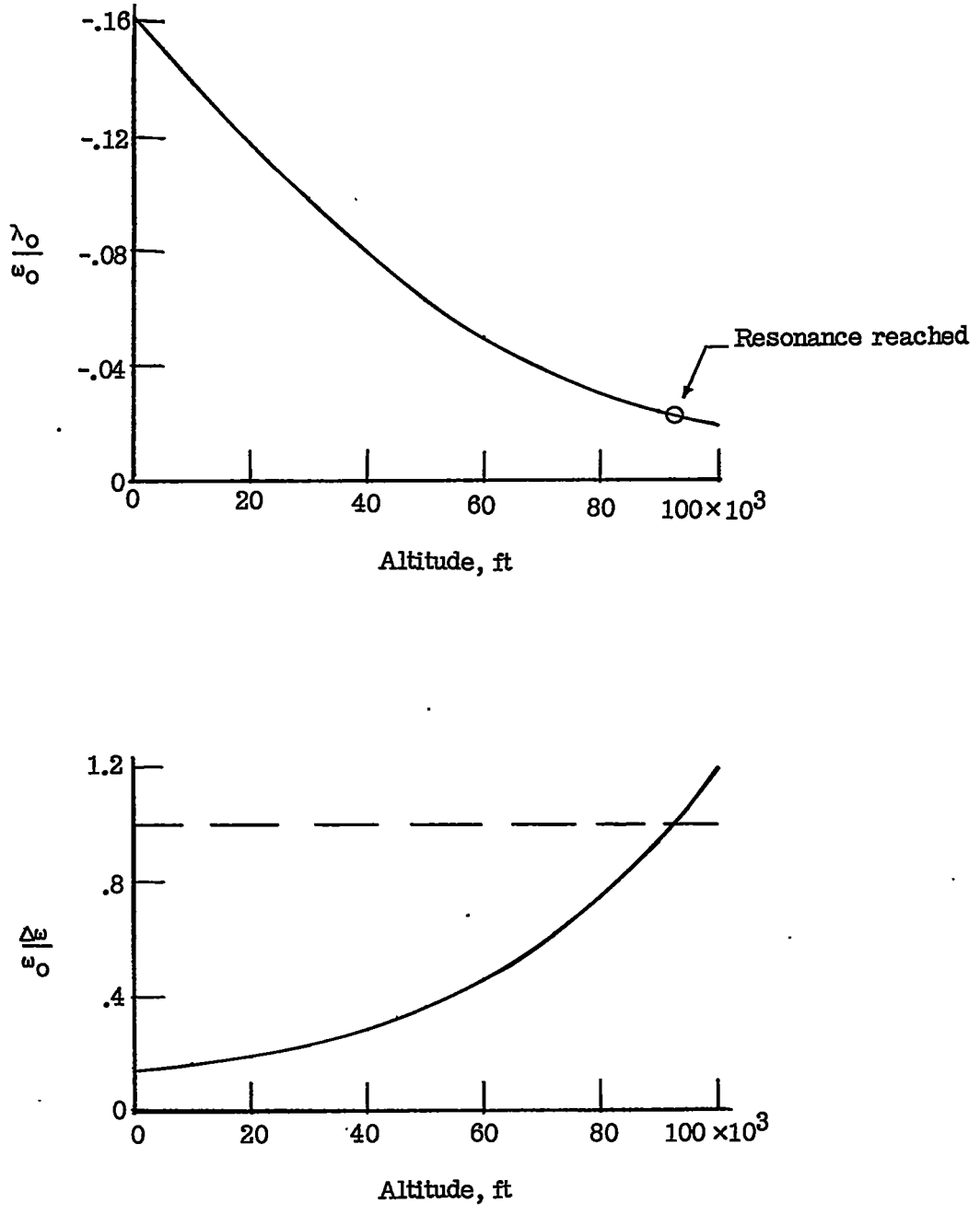

Figure 3.- Variation of λ_o/ω_o and $\Delta\omega/\omega_o$ with altitude for a high-speed missile. $C_{N_\alpha} = 3.65$; $\frac{dC_m}{dC_N} = -0.5$; $\frac{1}{2(k/d)^2}\frac{C_{m_q}}{C_{N_\alpha}} = -3$; $C_{n_{p_\alpha}} = 0$; $k/d = 2.60$; $4m/A_F d = 36.2$.

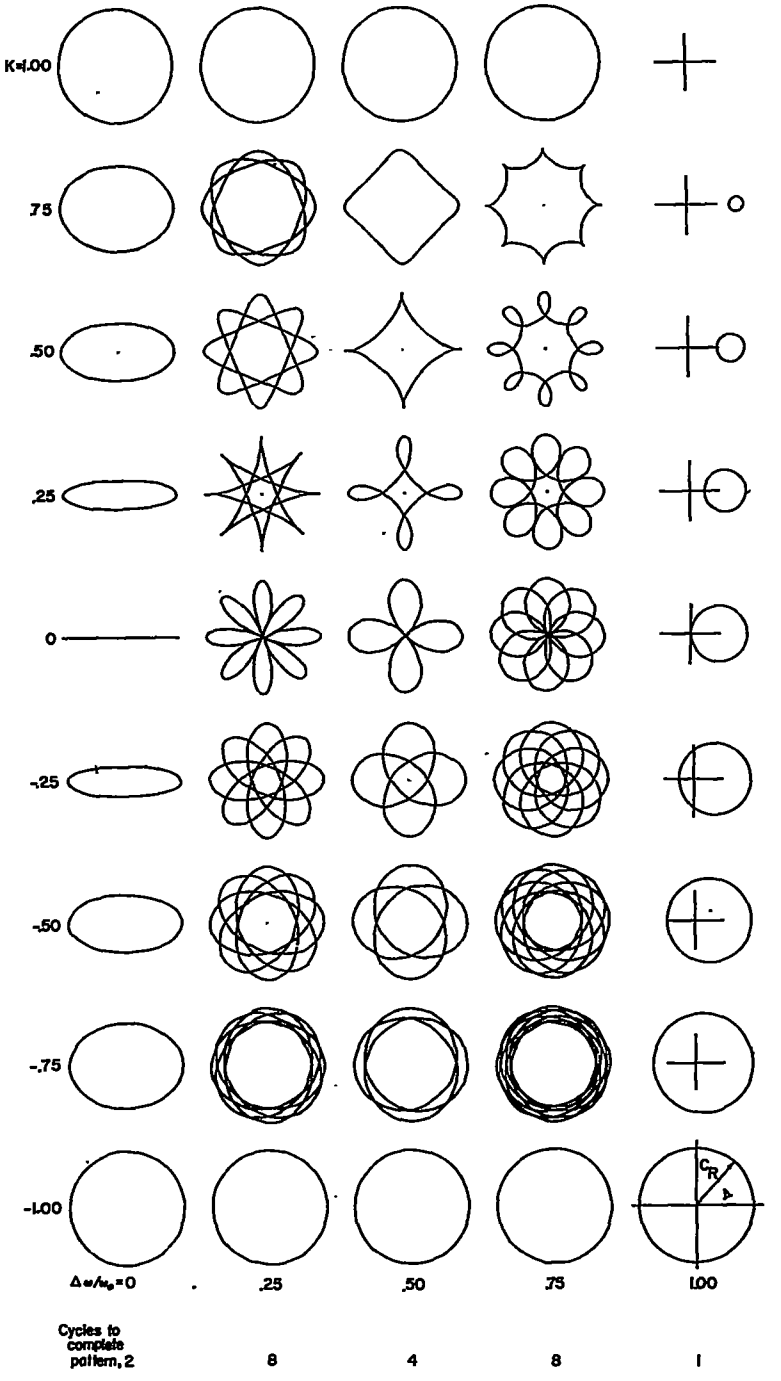

Figure 4.- Typical missile motions below roll resonance for $\Delta\omega/\omega_o$ positive. For negative values of $\Delta\omega/\omega_o$, the sign of K is reversed. $\lambda_o = \Delta\lambda = 0$.

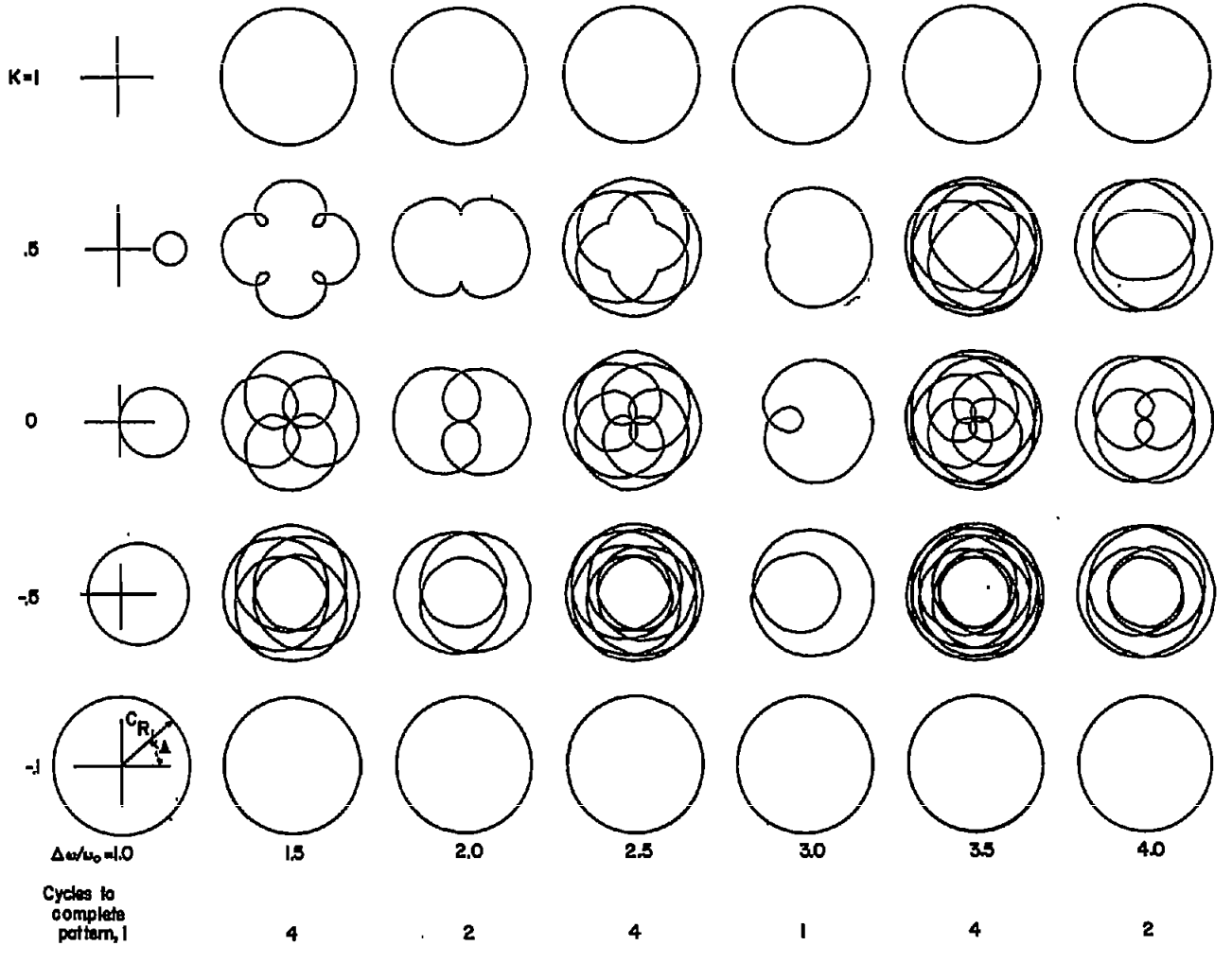

Figure 5.- Typical missile motions above roll resonance for $\Delta\omega/\alpha_o$ positive. For negative values of $\Delta\omega/\alpha_o$, the sign of K is reversed. $\lambda_o = \Delta\lambda = 0$.

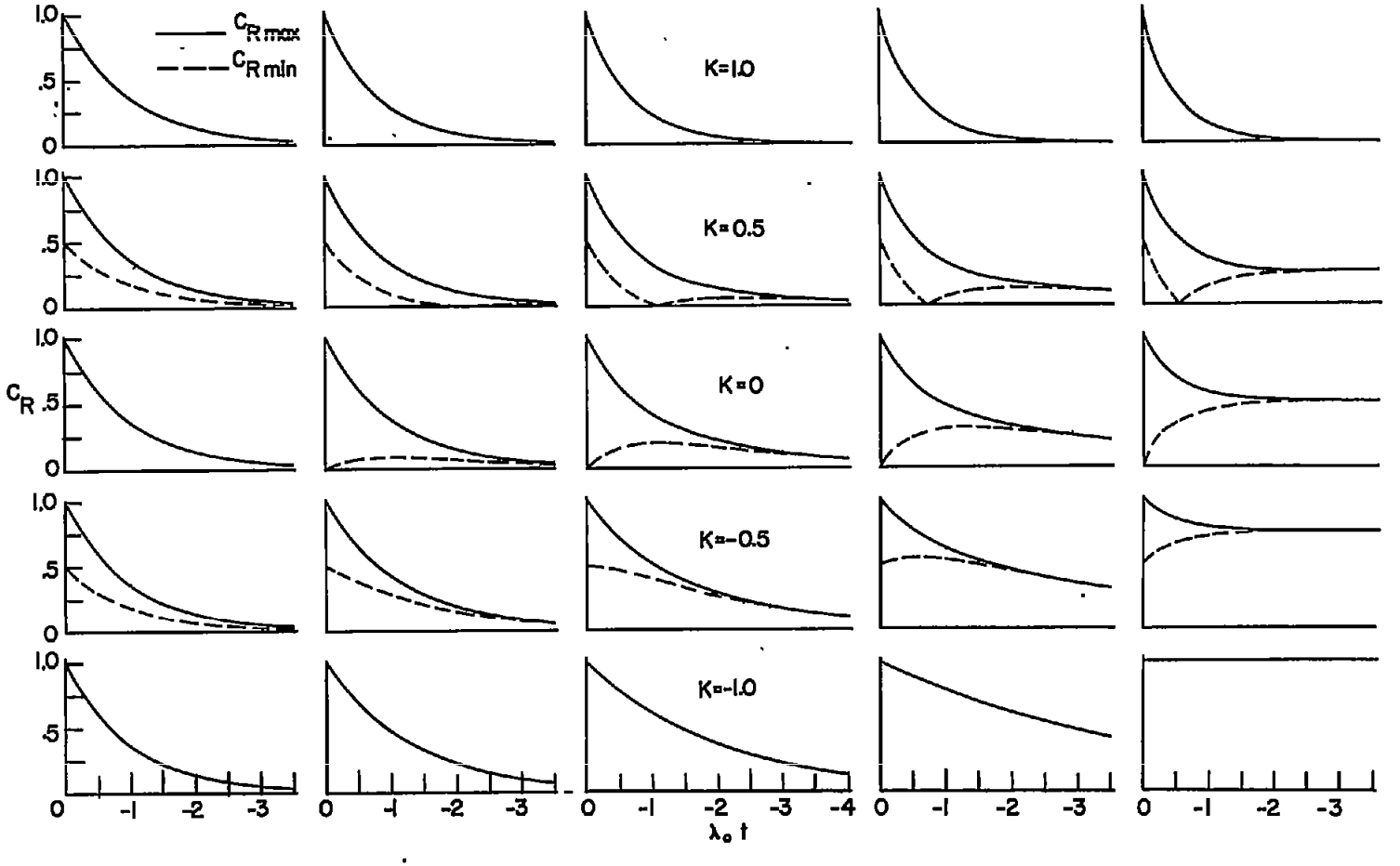

(a) $\frac{\Delta\lambda}{\lambda_o} = 0.$ (b) $\frac{\Delta\lambda}{\lambda_o} = 0.25.$ (c) $\frac{\Delta\lambda}{\lambda_o} = 0.50.$ (d) $\frac{\Delta\lambda}{\lambda_o} = 0.75.$ (e) $\frac{\Delta\lambda}{\lambda_o} = 1.00.$

Figure 6.- Envelopes of the C_R oscillations for $\Delta\lambda/\lambda_o$ positive. For negative values of $\Delta\lambda/\lambda_o$, the sign of K is reversed.

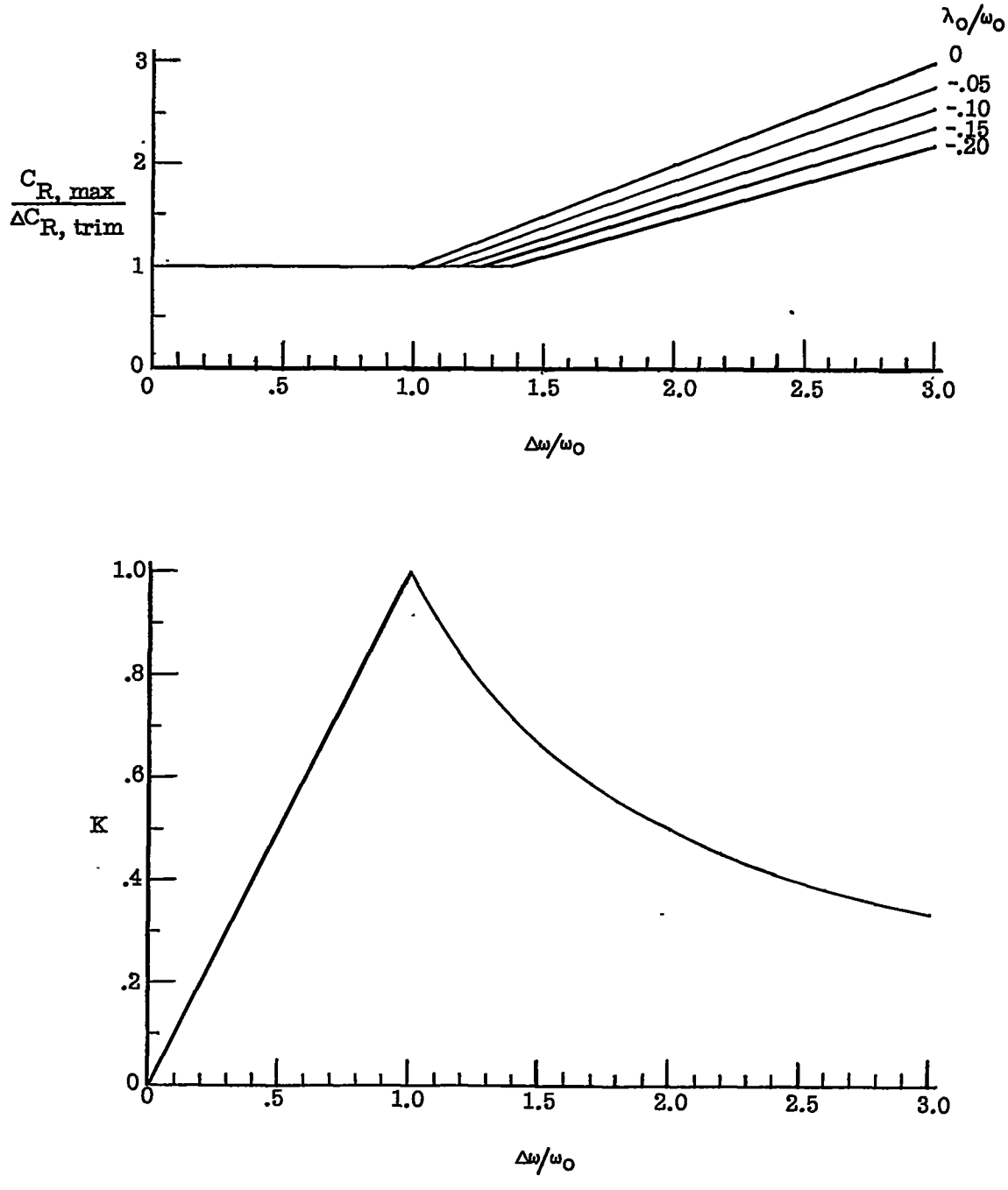

Figure 7.- Response of a rolling symmetrical missile to a trim change.

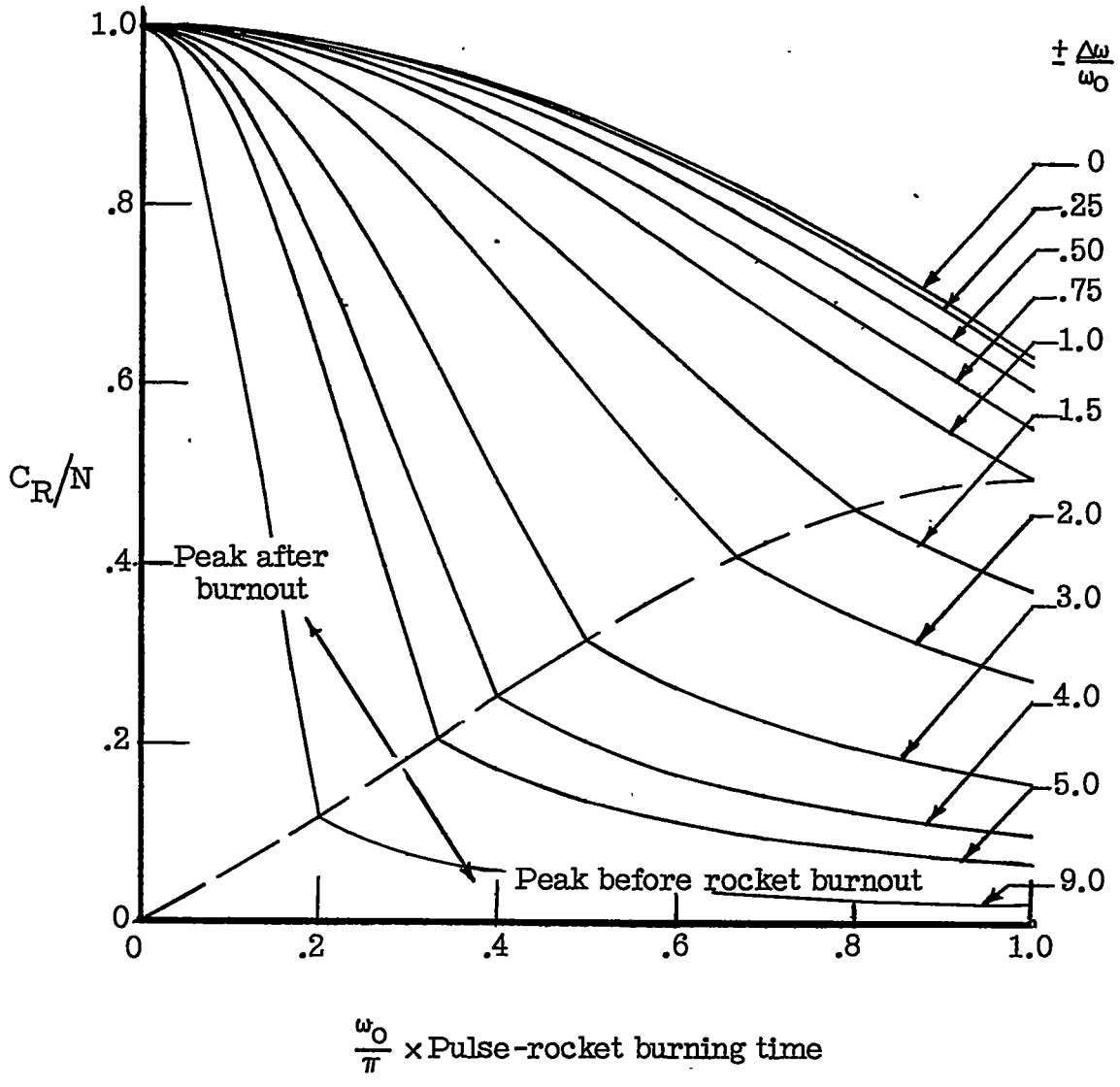

Figure 8.- Amplitude response of a rolling symmetrical missile to the disturbance from a pulse rocket having constant thrust. $\lambda_o = 0$; $\Delta\lambda = 0$; $N = \frac{Pd}{I\omega_o}\sqrt{\left(\frac{l}{d} + \frac{C_{m_{\dot{\theta}}}}{m'}\right)^2 + 4\left(\frac{k}{d}\right)^4\left(\frac{pd}{2V}\right)^2\left(1 - \frac{I_X}{I}\right)^2}$; C_R indicates resultant angle of attack.

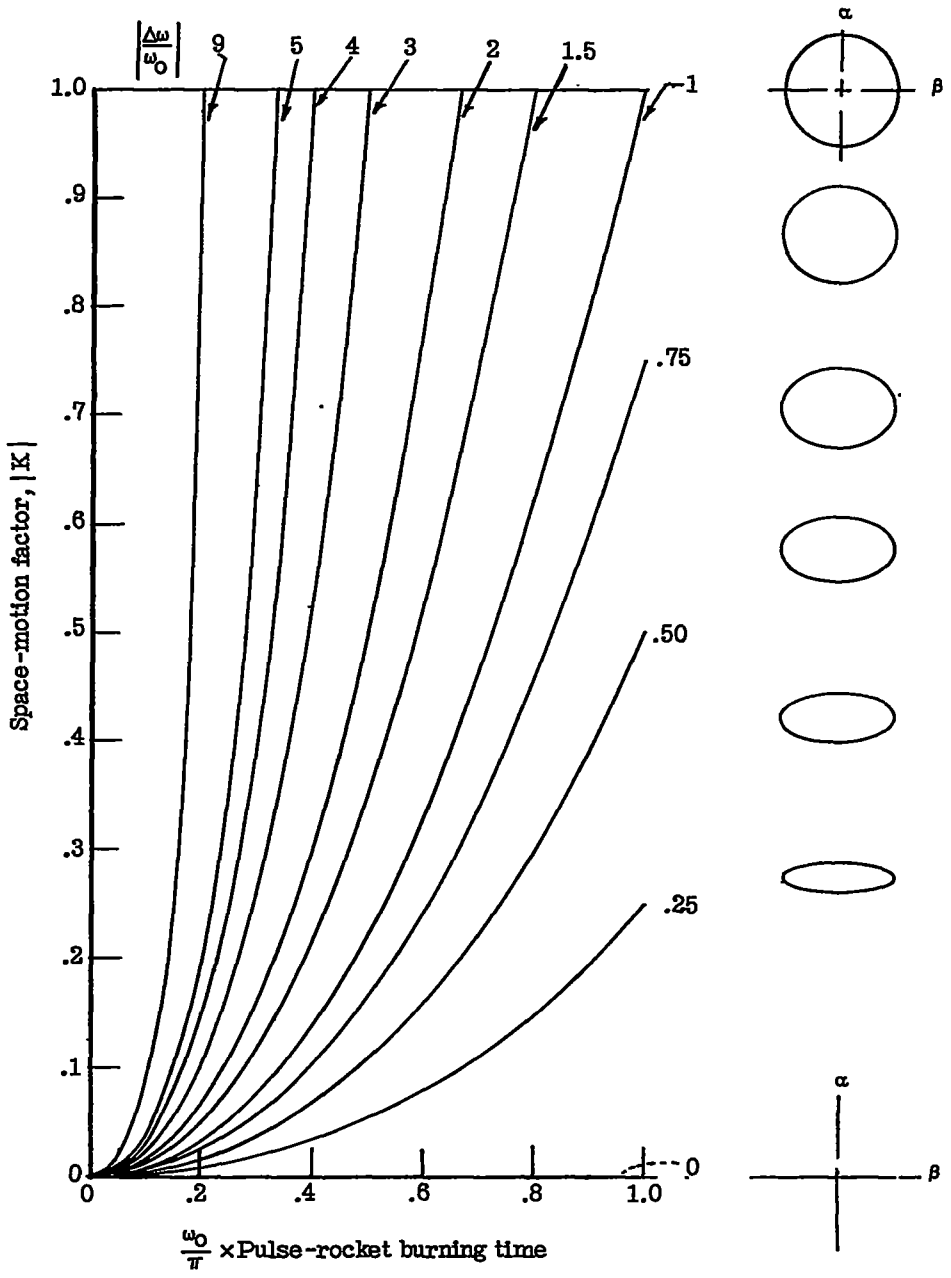

Figure 9.- Effect of pulse-rocket disturbance on the motion in space of a symmetrical missile. $\lambda_o = 0$; $\Delta\lambda = 0$. (K and $\frac{\Delta\omega}{\omega_o}$ have the same sign.)

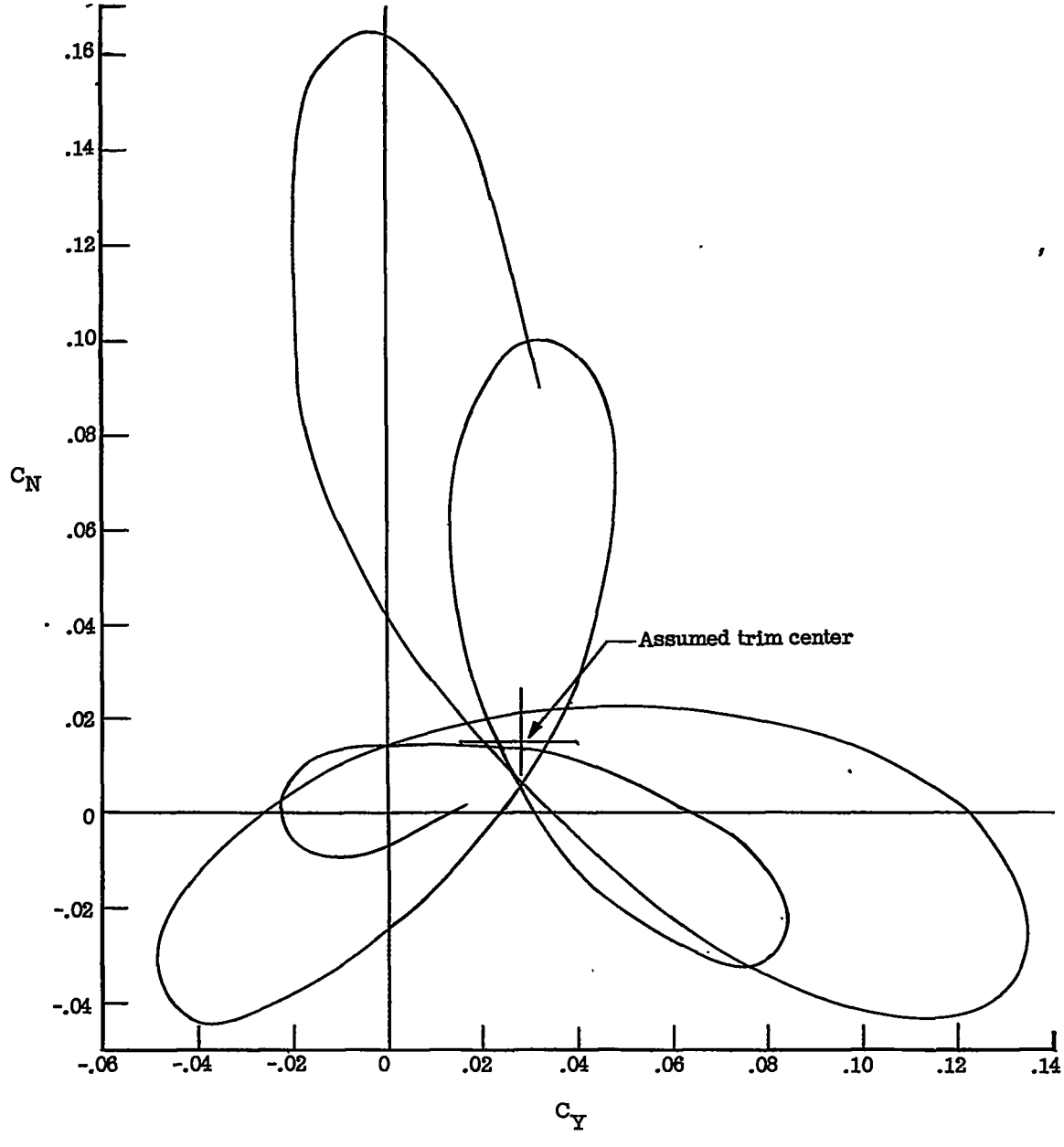

Figure 10.- Plot of C_N against C_Y for a rolling missile following a pulse-rocket disturbance.

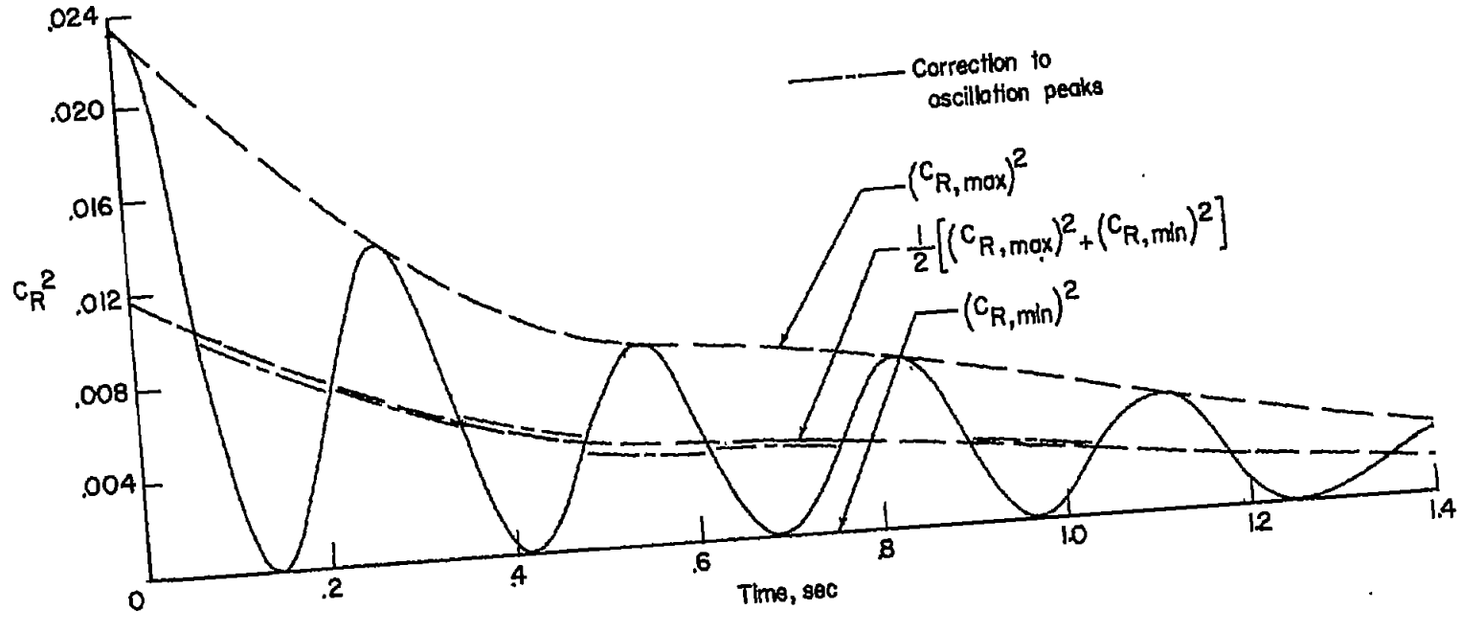

Figure 11.- Oscillation of C_R^2 from figure 10.

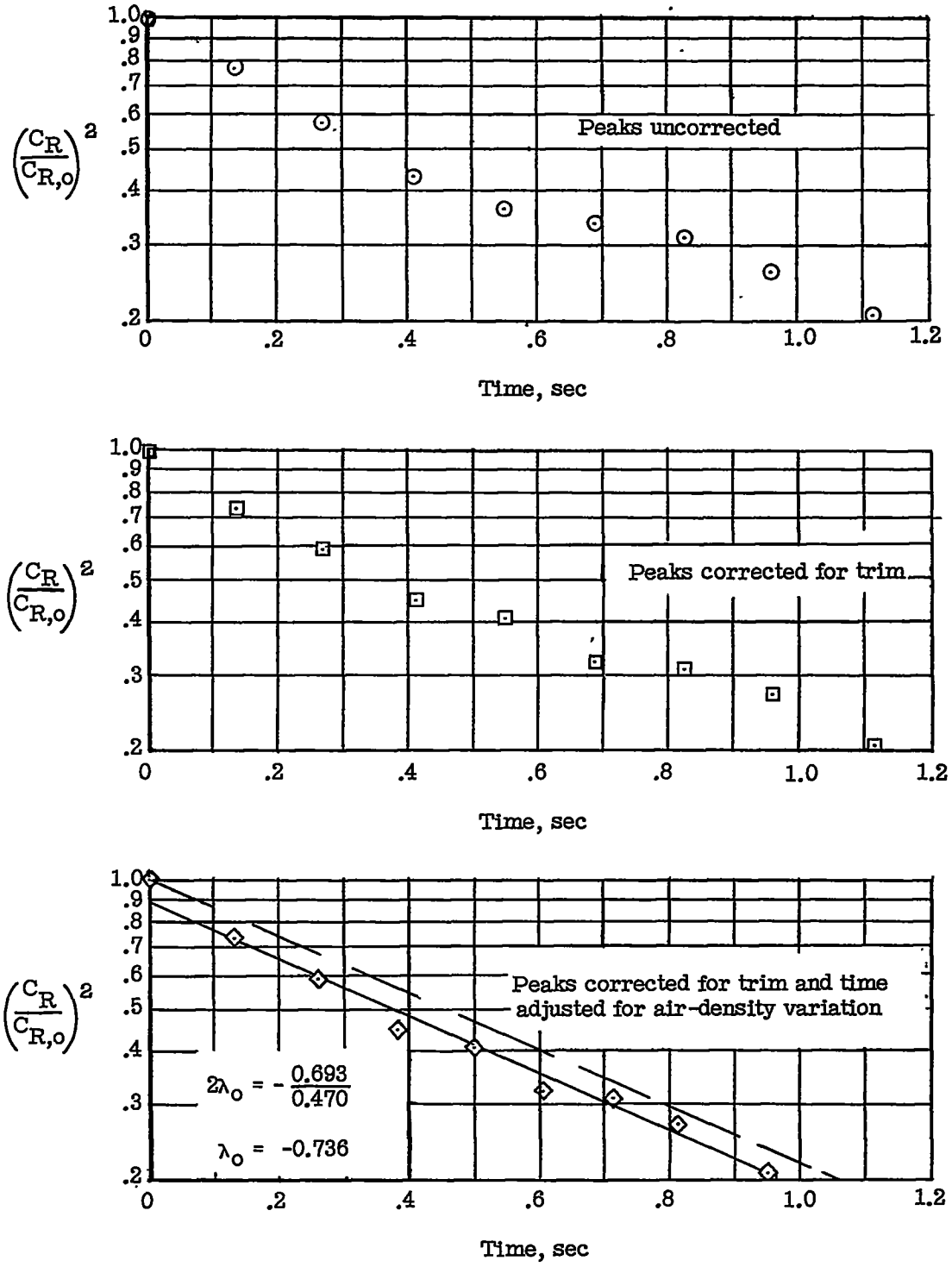

Figure 12.- Example of the determination of λ_o.

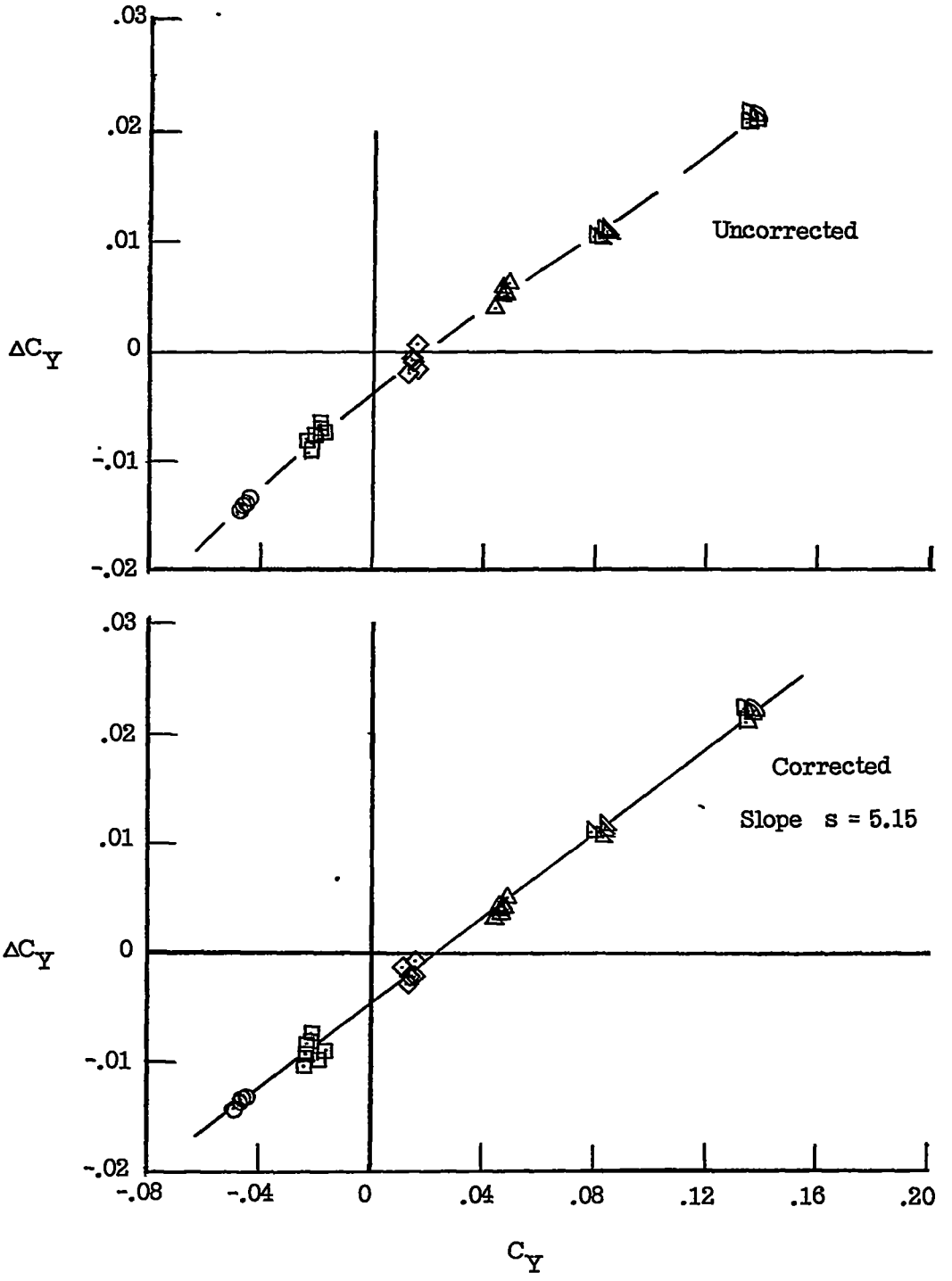

Figure 13.- Plot of ΔC_Y against C_Y.

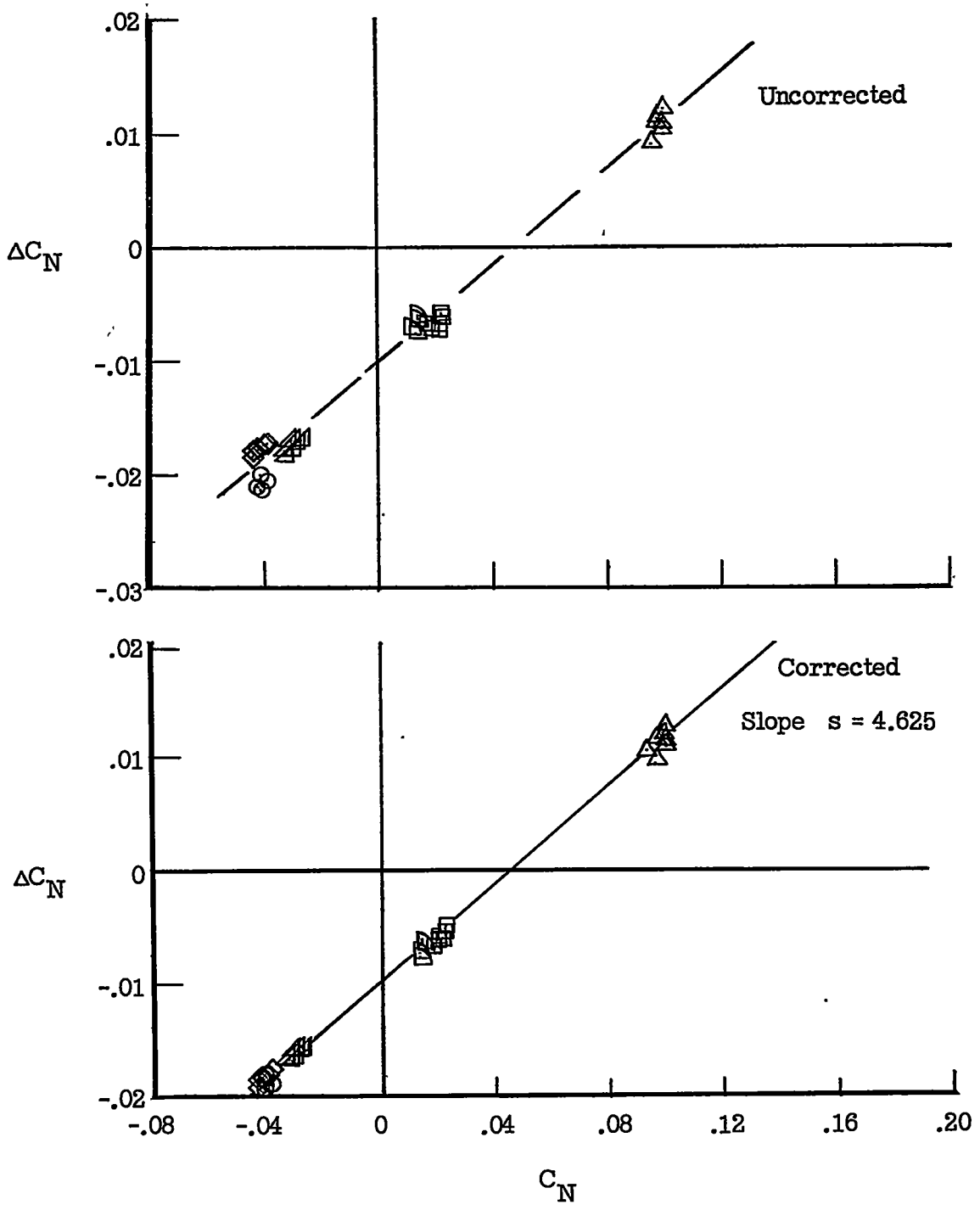

Figure 14.- Plot of ΔC_N against C_N.